INVESTIGATION OF β-LACTAMASE LIGAND BINDING *IN VIVO* AND *IN SILICO*

by

Pınar Kanlıkılıçer

B.S., Chemical Engineering, Yıldız Technical University, 2006

Submitted to the Institute for Graduate Studies in
Science and Engineering in partial fulfillment of
the requirements for the degree of
Master of Science

Graduate Program in Chemical Engineering
Boğaziçi University
2008

INVESTIGATION OF β-LACTAMASE LIGAND BINDING *IN VIVO* AND *IN SILICO*

APPROVED BY:

Prof. Amable Hortaçsu .....
(Thesis Supervisor)

Assist. Prof. Elif Özkırımlı Ölmez .....
(Thesis Co-Supervisor)

Assist. Prof. Burak Alakent .....

Prof. Betül Kırdar .....

Assist. Prof. Berna Sarıyar Akbulut .....

DATE OF APPROVAL: 12.01.2009

ACKNOWLEDGMENTS

I would like to express my gratitude to my thesis advisor and co-advisor, Prof. Amable Hortacsu and Assist. Prof. Elif Özkırımlı Ölmez, for their invaluable guidance, support and motivation during my MS thesis.

It is a pleasure for me to thank Assist. Prof. Berna Sarıyar Akbulut, not only for her continuous support and friendly encouragement throughout this research, but also for the unforgettable effort she has shown in reading and evaluating this work.

I would like to thank Assist. Prof. Burak Alakent for providing all of the MATLAB scripts used in this study and for the training in MATLAB and other computer skills.

I would also like to thank the members of my Examining Committee, Professor Betül Kırdar for reading and providing comments on my thesis.

I am grateful to Ezgi Akkaya and Yasemen Güngörmez for sharing all the good and bad times. They made the sleepless nights more enjoyable together. Very special thanks to my friends Hacer Güneş, Arman Basmacıoğlu, Elif Ercan and Banu Yavuztürk for giving me their everlasting friendship and joyful help. Finally, thanks are due to Mustafa Veysi Soyvural for making sure the thesis is well written with up-to-date standards.

Heartfelt thanks are for Nilay Büdeyri for her friendship and help throughout my studies.

And the biggest thanks are to my mother, Banu Gürel, father Ahmet Kanlıkılıçer, and my dear brother Alp Emre Kanlıkılıçer for their everlasting encouragement and support that they have shown to me. This thesis is dedicated to them.

Graduate student scholarship provided by TUBITAK and funding by BAP project 06A501 and 08A502 are gratefully acknowledged.

ABSTRACT

β-lactam antibiotics are the most commonly used antibiotics due to their high effectiveness, low cost, ease of delivery and minimal side effects. Bacteria have acquired resistance to these antibiotics. One of the mechanisms of acquired drug resistance is the bacterial production of beta-lactamases, which break down these antibiotics. Currently used beta-lactamase inhibitors are not effective at targeting the 700 types and new mutants of β-lactamases. β-lactamase inhibitor design is therefore an important research field. β-lactamase inhibitory protein (BLIP) of Streptomyces clavuligerus is a potent inhibitor of several β-lactamases. The research presented in this thesis aims to guide the design of new peptide inhibitors based on BLIP structures. Computational studies are performed to elucidate the mechanism of TEM-1 β-lactamase inhibiton by BLIP. To this end, molecular dynamics simulations of TEM-1 BLIP and TEM-1 peptide complexes were carried out. Asp49 residue on BLIP and the BLIP based peptide were mutated to determine the contribution of this residue to binding. Binding free energy of the TEM-1 BLIP and TEM-1 mutant BLIP (D49A) complexes were estimated by the molecular mechanics Poisson Boltzmann Surface Area method (MM-PBSA). The binding free energy of TEM-1 BLIP complex was lower than that of the TEM-1 mutant BLIP complex, which indicates the contribution of the Asp49 residue of BLIP to tight binding.

The experimental studies aimed to test the *in-vivo* BLIP – RTEM-1 β-lactamase binding and inhibition. The interaction of the two proteins was already verified using *in-vitro* studies however there was no report on their interaction under physiological conditions within the cells. For this purpose BLIP gene from *Streptomyces clavuligerus* was inserted into the pET20b(+) plasmid vector downstream from the pelB signal sequence and the recombinant protein was expressed in *E. coli* BL21(DE3). This signal sequence was required to direct BLIP to the periplasmic space where the RTEM-1 β-lactamase was located. The β-lactamase was expressed constitutively from the same plasmid. Upon induction with IPTG, cell growth was slightly retarded. This may be an evidence of the β-lactamase inhibition by BLIP and may provide preliminary results for further *in-vivo* experiments about BLIP β-lactamase binding.

ÖZET

β-lactam antibiyotikleri yüksek etki, düşük fiyat ve minimum yan etkilerinden dolayı en genel kullanılan antibiyotiklerdendir. Ancak bakteriler bu antibiyotiklere karşı direnç kazanmışlardır. Bu direnç mekanizmalardan bir tanesi de bakteri tarafından üretilen ve bu antibiyotikleri parçalayan β-laktamaz enzimidir. Şuan 700 tür ve yeni mutantlarına sahip β-laktamaz enzimlerine karşı kullanılan inhibitörlerin çok etkili olamamalarından dolayı β-laktamaz inhibitor tasarımı önemli bir araştırma alanıdır. *Streptomyces Clavuligerus*'un sahip oldugu β-laktamaz inhibitor proteini (BLIP) birçok β-laktamazı inhibe etme özelliğine sahiptir. Bu tezde sunulan araştırmanın BLIP'den yeni peptid inhibitor tasarımına ışık tutması amaçlamaktadır. Bilgisayar çalışmaları TEM-1 β-laktamazın BLIP tarafından inhibisyon mekanizmasının anlaşılmasına yöneliktir. Bu amaçla, TEM-1 BLIP ve TEM-1 peptid komplekslerinin moleküler dinamik çalışmaları yürütülmüştür. BLIP ve BLIP' den türetilen peptidlerde Asp 49 amino asidinin β-laktamaza bağlanmasındaki katkısını anlayabilmek için mutasyon yapılmıştır. TEM-1 - BLIP ve TEM-1 - BLIP (D49A) komplekslerinin serbest bağlanma enerjileri Moleküler Mekanik Poisson Boltzmann Yüzey Alanı metodu ile hesaplanmıştır. TEM-1 BLIP kompleksinin serbest bağlanma enerjisinin TEM-1 mutant BLIP kompleksin enerjisinden daha düşük çıkması Asp49 'un BLIP' e bağlanmasında önemli bir rol oynadığını gösterir.

Deneysel çalışmalar BLIP – RTEM-1 β-laktamazın hücre içinde bağlanma ve inhibisyonunu test etme amaçlıdır. İki molekülün birbiriyle etkileşimi daha önce yapılmış olan *in vitro* çalışmalarla doğrulanmıştır ancak fizyolojik koşullarda hücre içindeki etkileşimlerine dair rapor bulunmamaktadır. Bu amaçla *Streptomyces clavuligerus*' dan elde edilen BLIP geni pET20b(+) plasmid vektörüne PelB sinyal dizisinin önüne klonlanmıştır. Rekombinant protein *E.coli* BL21(DE3)' e ekspres edilmiştir. Sinyal dizisi, BLIP' in hücre içinde RTEM-1 β-laktamazın bulunduğu periplasmaya geçmesi için gerekli bir dizdir. β-laktamaz aynı plasmid tarafından yapısal olarak eksprese edilmiştir. IPTG indüksiyonundan sonra hücre büyümeleri hafif miktarda geciktirilmiştir. Bu sonuç BLIP' in β-laktamazı inhibe ettiğine dair bir delil olabilir ve daha sonraki in-vivo ortamda yapılacak BLIP- β-laktamaz bağlanma çalışmaları için ön sonuç temin edebilir.

TABLE OF CONTENTS

ABSTRACT iv
ÖZET v
LIST OF FIGURES ix
LIST OF TABLES xii
LIST OF SYMBOLS / ABBREVIATIONS xiv
1. INTRODUCTION 1
1.1. Biological Background 1
1.1.1. β-lactam Antibiotics and β-lactamase Mediated Antibiotic Resistance 1
1.1.2. β-Lactamase Structure 3
1.1.3. Tem-1 β-lactamase 4
1.1.4. β-Lactamase Inhibitory Protein 5
1.2. Recent Research on TEM-1 β-lactamase Ligand Recognition 9
1.3. Objectives and Plan of the Study 10
2. COMPUTATIONAL METHODS 11
2.1. Simulation Systems 11
2.2. Molecular Dynamics Simulations 12
2.2.1. Force Field 13
2.2.2. NAMD 14
2.2.3. Simulation Parameters 15
2.3. Trajectory Analysis 16
2.3.1. Root Mean Square Deviations 16
2.3.2. Mean Square Fluctuations of Positions 16
2.3.3. PCA Analysis 16
2.4. Binding Fee Energy Calculations 17
2.4.1. Molecular Mechanics Poisson Bolztmann Surface Area (MMPBSA) 17
3. COMPUTATIONAL RESULTS 19
3.1. Root Mean Square Deviations from Initial Structure 19
3.1.1. Tem-1 β-lactamase 20
3.1.2. β-lactamase Inhibitory Protein 22

3.2. Mobility and Flexibility of Structures from MD Simulation Trajectories 24
3.2.1. Wild type TEM-1 β-lactamase 24
3.2.2. TEM-1 – BLIP Complex 26
3.2.3. TEM-1 – Mutant BLIP Complex 27
3.2.4. TEM-1 – Peptide Complexes 29
3.3. Effect of D49A mutation on BLIP on TEM-1 structure and binding 31
3.4. Important Residue Interactions 33
3.4.1. Ser 70 – Lys 73 33
3.4.2. Ser 70 – Ser130 34
3.4.3. Ser 70 – Lys234 35
3.5. Binding Free Energy Calculations 37
4. EXPERIMENTAL METHODS 38
4.1. Cloning of BLIP gene 38
4.1.1. Extraction of genomic DNA 38
4.1.2. Amplification of BLIP gene 38
4.1.3. Purification of PCR products (BLIP gene)..... 39
4.1.4. Restriction Enzyme Digestion..... 40
4.1.4.1. pET 20 b(+) Plasmid Digestion with restriction enzymes……..... 40
4.1.4.2. BLIP Digestion with restriction enzymes…….. 40
4.1.5. DNA purification from restriction reactions 40
4.1.6. Ligation of the BLIP gene and the pET20b(+) plasmid 41
4.2. Transformation of pET20b(+) into *E.coli* by $CaCl_2$ 41
4.3. Plasmid isolation 42
4.3.1. Mini-Prep Plasmid Isolation 42
4.4. Restriction enzyme digestion for screening recombinant colonies 43
4.5. Agarose Gel Electrophoresis of DNA 43
4.6. Growth of Recombinant *E. coli* Cells and Expression of Recombinant Proteins …… 44
5. MATERIALS 45
5.1. Bacterial Strains and Plasmids 45
5.2. Chemicals and Enzymes 45
5.3. Laboratory Equipments 45
5.4. Growth Media for *Escherichia coli* 46

5.5. Buffers and Solutions 46
5.6. Kits 47
6. RESULTS AND DISCUSSION 48
6.1. Cloning of BLIP gene 48
6.1.1. Pimer Design 50
6.1.2. Optimization of PCR conditions 51
6.2. Screening of the Recombinant Colony 52
6.3. Expression of the BLIP gene 53
7. CONCLUSIONS AND RECOMMENDATION FOR FUTURE STUDIES..... 55
7.1. Conclusions..... 55
7.2. Recommendations for Future Studies..... 57
APPENDIX A: INPUT FILES USED IN COMPUTATIONAL STUDIES..... 58
APPENDIX B: RESIDUE– RESIDUE DISTANCES IN THE MD SIMULATIONS.... 71
APPENDIX C: MMPBSA RESULTS 73
REFERENCES 77

LIST OF FIGURES

Figure 1.1. β-lactam amide bond breakdown 2

Figure 1.2. Representation of BLIP bound to TEM-1 β-lactamase. 6

Figure 1.3. Representation of TEM-1 the region of BLIP from residues 99 to112 8

Figure 1.4. Representation of BLIP binding to TEM-1 β-lactamase 9

Figure 2.1. Structure of the TEM-1 β-lactamase - HAAGDYYA peptide complex 11

Figure 2.2. Structure of the TEM-1 β-lactamase - FYRGSAHLWFY peptide complex 12

Figure 3.1. Root Mean Square Deviation of Apo TEM-1 β-lactamase 20

Figure 3.2. RMSD of TEM-1 β-lactamase in TEM-1 – BLIP and TEM-1 – BLIP (D49A) complex 21

Figure 3.3. RMSD of the Cα atoms of TEM-1 β-lactamase complexes with peptides … 22

Figure 3.4. BLIP and Mutant BLIP RMSD 23

Figure 3.5. RMSD profiles of BLIP in apo BLIP, TEM-1 BLIP and TEM-1 - mutant BLIP (D49A) complex 23

Figure 3.6. RMSD profiles of the peptides 24

Figure 3.7. MSF of TEM-1 β-lactamase …….. 25

Figure 3.8. TEM-1 β-lactamase mobility for the unbound enzyme..... 25

Figure 3.9. MSF of TEM-1 β-lactamase in TEM-1 - BLIP complex.simulation 26

Figure 3.10. TEM-1 β-lactamase mobility in TEM-1-BLIP complex …….…..... 27

Figure 3.11. MSF of TEM-1 β-lactamase in TEM-1 – mutant BLIP (D49A)

simulation …….. 28

Figure 3.12. TEM-1 β-lactamase mobility in TEM-1 - BLIP (D49A) complex 28

Figure 3.13. MSF of TEM-1 β-lactamase in TEM-1 - peptide complex simulations 29

Figure 3.14. TEM-1 β-lactamase mobility in TEM-1 - peptide (HAAGDYYA) 30

Figure 3.15. TEM-1 β-lactamase mobility in TEM-1 – peptide (HAAGAYYA) 30

Figure 3.16. TEM-1 β-lactamase mobility in TEM-1 – peptide (FYRGSAHLWFY) 31

Figure 3.17. Effect of D49A mutation on TYR105 residue of TEM-1 β-lactamase 32

Figure 3.18. Ser 70 and Lys 73 active site residue interaction of TEM-1

β-lactamase 34

Figure 3.19. Ser 70 and Seri 130 active site residue interaction of TEM-1

β-lactamase 35

Figure 3.20. Ser70 and Lys 234 active site residue interaction of TEM-1 β-lactamase 36

Figure 6.1. pET20-b(+) plasmid vector 49

Figure 6.2. Electrophoretic analysis of amplified BLIP on agarose gel 51

Figure 6.3. Electrophoretic analysis of of the double digested BLIP gene and the linearized pET20b(+) plasmid on agarose gel 52

Figure 6.4. Electrophoretic analysis of the isolated recombinant colony on agarose gel……... 53

Figure B.1. Ser70 - Ser130 active site residue distances of TEM-1 – BLIP complexes…… 71

Figure B.2. Ser70 - Ser130 active site residue distances of TEM-1 – Peptide complexes…… 71

Figure B.3. Ser70 – Lys234 active site residue distances of TEM-1 – BLIP complexes ……... 72

Figure B.4. Ser70 – Lys234 active site residue distances of TEM-1 – Peptide complexes…… 72

LIST OF TABLES

Table 1.1. Important residues of TEM-1 β-lactamase in terms of ligand binding 5

Table 1.2. The interacting residues on TEM-1 beta lactamase and BLIP 7

Table 3.1. RMSD values of TEM-1 beta lactamase 19

Table 3.2. RMSD values of BLIP or peptides 20

Table 3.3. Distances between the active site residues(S70, K73, S130, E166, K234) of TEM-1 β-lactamase 33

Table 3.4. Binding Free Energy components of TEM-1 - BLIP complex and TEM-1 mutant BLIP complex simulations obtained by APBS 37

Table 4.1. Primers used for the amplification of BLIP gene 39

Table 5.1. List of Laboratory Equipments 45

Table 5.2. LB Medium 46

Table 5.3. LB Agar Medium 46

Table 5.4. 10X TBE Buffer 46

Table 6.1. Specification of designed primers 50

Table C.1. Apolar Energy Values of TEM-1 - BLIP and TEM-1 - BLIP (D49A) complexes 73

Table C.2. Polar Energy Value of TEM-1 - BLIP Complex 73

Table C.3. Polar Energy Values of TEM-1 - BLIP (D49A) Complex 73

Table C.4. Coulomb Energy Values of TEM-1 - BLIP Complex 74

Table C.5. Coulomb Energy Values of TEM-1 - BLIP (D49A) Complex 74

Table C.6. Internal Energy Values of TEM-1 - BLIP Complex 74

Table C.7. Internal Energy of Values TEM-1 - BLIP (D49A) Complex 75

Table C.8. Van der Waals Energy Values of TEM-1 - BLIP Complex 75

Table C.9. Van der Waals Energy Values of TEM-1 - BLIP (D49A) Complex 75

Table C.10. Delta Energy Values of TEM-1 – BLIP Complex 76

Table C.11. Delta Energy Values of TEM-1 – BLIP (D49A) Complex 76

LIST OF SYMBOLS / ABBREVIATIONS

a_i	Acceleration of particle *i*
F_i	Force acting on particle *i*
M_i	Virtual bond vector of particle *I*
MW	Molecular weight
Da	Dalton
K_i	Inhibition constant
K_φ	Dihedral force constant
k_w	Force constant
k-Da	kilo dalton
m_i	Mass of particle *i*
nM	nanomolar
ns	nanosecond
R_i	Position of particle *i*
V	Potential energy
Å	Angstrom
φ	dihedral angle
A	Ala, Alanine
BLIP	Beta-lactamase Inhibitory Protein
D	Asp, Aspartic acid
E	Glu, Glutamine acid
F	Phe, Phenylalanine
FITR	Fourier Transform Infrared
G	Gly, Glycine
H	His, Histidine
K	Lys, Lysine
L	Leu, Leucine
MD	Molecular Dynamics
MM PBSA	Molecular Mechanics Poisson Boltzmann Solvent Accessible Surfa Area

MSF	Mean Squared Fluctuation
N	Asn, Asparagine
OD	Optical Density
P	Pro, Proline
PCA	Principal Components analysis
PDB	Protein Data Bank
PME	Particle Mesh Ewald
R	Arg, Arginine
RMSD	Root mean squared deviation
Q	Gln, Glutamine
S	Ser, Serine
T	Thr, Threonine
V	Val, Valine
VDW	van der Waals
W	Trp, Tryptophan
Y	Tyr, Tyrosine
3-D	Three-dimensional

1. INTRODUCTION

1.1. Biological Background

1.1.1. β-lactam Antibiotics and β-lactamase Mediated Antibiotic Resistance

β-lactams are the most commonly used antibiotics owing to their relatively high efficiency, simplicity of deliverance, little cost, and minimum side effects. β-lactams targets transpeptidase enzymes which are responsible for the synthesis of the bacterial cell wall. Eventually, the low cost of production of β-lactam antibiotics provides a broad availability; as a consequence, it is worth to consider them as a powerful clinical resource. The first β-lactam antibiotic which was presented into medical applications was penicilin (Babic et al., 2006).

β-lactam antibiotics such as penicillins and the cephalosphorins are efficient substrate-analogue-based pharmaceuticals, They target the bacterial cell-wall synthetic enzymes and kill bacteria (Strynadka et al., 1992). In order to maintain cell shape and solidity, a strong cross-linked peptidoglycan layer is utilized by all species of bacteria. A basic unit of repeating disaccharide - N-acetyl glucosamine andn-acetyl muramic acid - composes this cell wall. A characteristic pentapeptide changes the next sugar in the disaccharide which varies between gram-negative and gram-positive species, however finalizes with two D-alanine residues in each case. Each peptidoglycan units are formed within the cell, though the cell wall transpeptidases which is a group of membrane anchored bacterial enzymes, catalyzes their last crosslinking outside of the cytoplasmic membrane (Wilke et al., 2005)

The active-site serine residue of the transpeptidase is acylated by penicillins, cephalosphorins and related β-lactam antibiotics, composing a more stable covalent acylenzyme which is non-catalytic (Frére, 1995).

Unfortunately, bacteria have developed sophisticated resistance mechanisms to combat the lethal effects of these antibiotics. The most common mechanism is the production of enzymes that degrade or modify the antibiotics before they can reach the appropriate target sites. The β-lactamase family of enzymes degrades β-lactam antibiotics by hydrolysis of the amide bonds of the four-membered β-lactam ring. The spread of β-lactamase genes have been aided by their integration with mobile genetic elements such as plasmids or transposons. In gram-negative bacteria β-lactamase enzymes are secreted into the periplasmic space while in gram-positive bacteria these enzymes are bound to the cytoplasmic membrane or excreted to the medium. There are four classes (A-D) of β-lactamases based on primary sequence homology. Three of these classes (A, C and D) are serine active site enzymes and one class (B) use coordinated zinc ion as the reactive nucleophile. Class A enzymes are usually plasmid mediated, prefer penicillins as substrates and representative enzymes include TEM-1 and SHV (Wilke et al., 2005).

One of the serious and thriving problems in antibacterial treatment is antibiotic resistance of bacteria. β-lactamases and especially the class A family of these enzymes are the most common form of resistance against the very important group of β-lactam antibiotics. The β-lactam amide bond breakdown occurs in two major stages as outlined in Figure 1.1. The initial stage is that the antibiotic acylates Ser70 to form an acylenzyme intermediate. In the next step the acylenzyme (AE) is hydrolysed (deacylation). The former β-lactam compound is then released. Based on the antibiotic both acylation or deacylation can be the rate-determining step for the entire enzymatic reaction (Hermann et al., 2006).

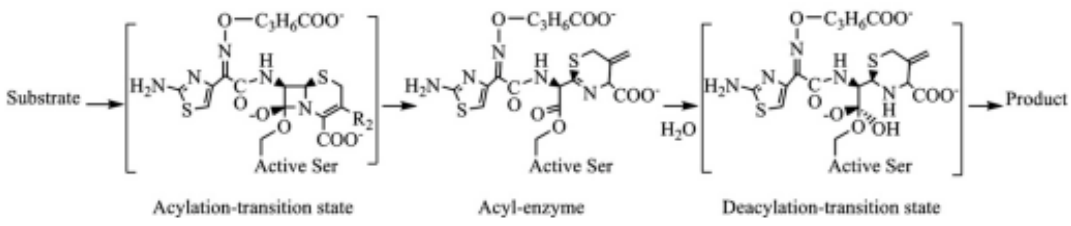

Figure 1.1. β-lactam amide bond breakdown (Delmas et al., 2008)

To overcome the antibiotic resistance mechanism mediated by β-lactamases, small molecule β-lactam inhibitors, such as clavulanic acid, cefotaxime and ceftazidime have been used. This approach, however, has applied selective pressure for mutations that result

in β-lactamases no longer sensitive to β-lactamase inhibitors. The structural information from BLIP·β-lactamase complex has been recently used to design novel peptide inhibitors (Rudgers et. al., 2001). The aim of this project is to design peptide inhibitors based on the BLIP structure.

1.1.2. β-Lactamase Structure

The class A, C and D β -lactamase enzymes are assumed to have come out from the same ancestral enzyme because of their structural similarity with the target of β-lactam antibiotics (Ghuysen, 1994). Class A β-lactamase from *Staphylococcus aureus* PC1 was used for the determination of the first β-lactamase crystal structure (Herzberg and Moult, 1987). Since then, approximately 80 structures of wild-type β-lactamases, mutant β-lactamases, and co-crystal structures of β-lactamase with substrate or inhibitor have been resolved. Close to half of these structures are for class A β-lactamase enzymes and class A β-lactamases are the most studied group.

S70-X-X-K, S130-X-N, K234-T/S-G, and the Ω-loop are four motifs which are found in the near of the active-site pocket of class A β-lactamases. S70-X-X-K motif comprises the active-site serine at position 70 and a lysine at position 73 (B-lactam numbering is due to Ambler, 1980). The general mechanism of class A β-lactamases involves the nucleophilic attack by Ser70, after activation by either Lys73 or Glu166, on the carbonyl carbon of the β-lactam ring resulting in the acyl-enzyme intermediate. An acyl-enzyme intermediate for class A β-lactamases was first identified by Fourier transform infrared (FTIR) spectroscopy (Fisher et al., 1980). Mutagenic studies replacing the active-site serine with other amino acids, including the closely related Thr residue, resulted in an inactive enzyme, clearly indicating that Ser70 is involved in hydrolysis of the β-lactam antibiotic (Chen et al., 1996; Dalbadie-McFarland et al., 1982, 1986; Ma-zella et al., 1991).

1.1.3. Tem-1 β-lactamase

Among the class A β-lactamases, TEM-1 (263 residues, MW 28907 Da) is the most commonly found and is responsible for the resistance to β-lactam antibiotics of various pathogenic bacteria. Plasmids and transposable elements have carried out a large amount of genetic dissemination of β-lactamase. TEM-1 is the most frequently observed plasmid-mediated β-lactamase and has contributed notably to resistance against β-lactam antibiotics (Majiduddin et al., 2002). Clinical isolates of infectious bacteria have been used to identify more than 90 types of TEM-1 (Hujer et al., 2001).The hydrolysis of the amide bond in the β-lactam ring of antibiotics comprising the commonly used penicillins and cephalosporins is catalyzed very effectively by TEM-1 enzyme. The catalytic mechanism and the precise function of the active site residues are still disputable and the relationship between variations and their catalytic properties are not yet wholly explained in spite of the large amount of data acquired by a variety of techniques such as X-ray crystallography (Minasov et al., 2002; Strynadka et al., 1992) or molecular dynamics simulations (Diaz et al., 2003).

Strynadka et al. (1992) and then Jelsch et al. (1993) solved the X-ray crystal structure of TEM-1 β-lactamase. Mutagenesis studies as well as structural studies have elucidated residues important for the catalytic activity and binding of TEM-1 β-lactamase. Some of these residues are listed in Table 1.1. Two positions near the active site that have been altered due to the selective pressure imposed on them are Arg164 and Gly238. A salt bridge composed between Arg164 and Asp179 stabilizes the omega loop in TEM-1 β-lactamase (Jelsch et al., 1993; Kuzin et al., 1999). The substrate profile of the enzyme can be changed by disrupting the salt bridge between Arg164 and Asp179. Serine at position 238 boosts the TEM-1-catalyzed hydrolysis of cefotaxime is shown by mutagenesis studies and kinetic analysis (CantuIII et al., 1996; Venkatachalam et al., 1994). Through kinetic analysis of several TEM-1 variants at position 238, it was determined that the Ser side chain allowed for hydrogen bonding to another site within the enzyme, in contrast to the substrate (Cantu III and Palzkill, 1998).

Table 1.1. Important residues of TEM-1 β-lactamase in terms of ligand binding

Region	Function	Reference
Active site residues: S70,L73,S130,E166,N170,K234	Substrate catalysis	Jelsch et al.,1993
Omega loop: Residues 164 to 179	Forms the bottom wall of the active site pocket.	Strynadka et al.,1992.
E104, Y105	Substrate binding	Petit et al.,1995, Doucet et al.,2004.

A covalent acyl-enzyme intermediate is formed with the serine nucleophile in the double in-line displacement mechanism of TEM-1 β-lactamas (Cohen & Pratt, 1980; Joris, 1984; Knott-Hunziker et al., 1982). Ser70 is deprotonated for nucleophilic attack on the carbonyl C atom of the β-lactam ring either through its strong hydrogen bond to Lys73 or a water-mediated interaction to Glu166 in the acylation stage (Matagne & Frere, 1995; Matagne et al., 1998). Glu166 has been suggested to be the main general base in the reaction (Damblon et al., 1996) and high-resolution structural data (Minasov et al., 2002). The proximity of the Lys73 amine group suggests that it must also contribute in the deprotonation stage of Ser70. This proton is back-donated to the leaving N atom of the β-lactam ring through a hydrogen-bond network in the active site with the participation of Ser130. Activated water hydrogen bonded to Glu166 completes deacylation of this acyl-seryl intermediate (Adachi et al., 1991). The oxyanion hole which polarizes the carbonyl groups for nucleophilic attack in both acylation and deacylation and stabilizes the tetrahedral transition states in both stages is formed by the backbone amide groups of Ser70 and Ala237 (Fig. 2) (Stec et al., 2005).

More information on the mechanism of action of these proteins is required as resistant strains are still appearing concomitantly with the development of new antibiotics and β-lactamase inhibitors (Pierre-Yves et al., 2004).

1.1.4. β-Lactamase Inhibitory Protein

The increase in antibiotic resistance due to of β-lactamase production has made the development of novel inhibitors to these enzymes an area of intense research interest. β-lactamase inhibitory protein (BLIP) is a 17-kDa protein produced by *Streptomyces*

clavuligerus that inhibits class A β-lactamases with a wide range of affinities (Zhang and Palzkill, 1999). BLIP has been shown to be a potent inhibitor of class A β-lactamases from both gram-positive and gram-negative bacteria, including TEM-1 β-lactamase (K_i= 0.1 nM) (Petrosino et al., 1999).

The small molecule, β-lactamase inhibitor, clavulanic acid, was primarily purified from the soil bacterium *Streptomyces clavuligerus* (Reading and Cole, 1977).

BLIP is composed of two tandemly linked 76-amino acid domains. The complex structure between TEM-1 and BLIP has shown that BLIP binds to a negatively charged loop-helix region composed of residues 99–112 just outside the active site pocket of TEM-1 β-lactamase (Figure 1.3.A) (Rudgers and Palzkill, 1999).

Sequence alignments of class A β-lactamases which are inhibited by BLIP do not present a significant amino acid sequence conservation along 99-112 loop region (Strynadka et al., 1996). The interaction area between BLIP and β-lactamase (2636 $Å^2$) is one of the largest among known protein-protein interactions (Strynadka et al., 1996). The TEM-1·BLIP complex has therefore been used as a model system in many studies (Figure 1.2) (Zhang and Palzkill, 2003, 2004; Rudgers and Palzkill, 1999; Selzer et. Al, 2000).

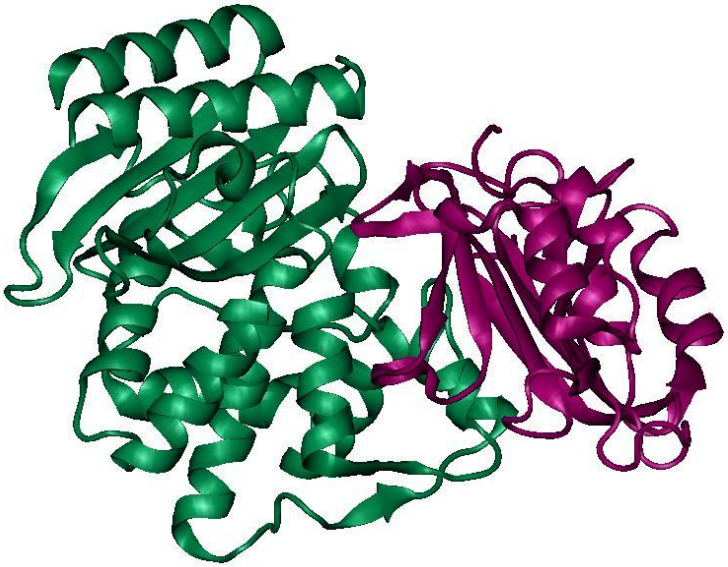

Figure 1.2. Cartoon representation of BLIP (magenta) bound to TEM-1 β-lactamase (green).

Table 1.2. The interacting residues on TEM-1 beta lactamase and BLIP

BLIP	**TEM-1 β-LACTAMASE**	**Reference**
Asp 49	Ser 130, Lys 234, Ser 235, Arg 244.	Petrosino et al.,1999
Phe 142	Glu104, Tyr 105, Asn 170, Ala 237, Gly 238, Glu240	Petrosino et al.,1999
Lys74	Glu104	Zhang et al.,2004.
Tyr 50	Pro 107, Val 216Met 129,	Zhang et al.,2003.
Glu 73	Glu104,Tyr105,Ser106	Zhang et al.,2003.
Loop 1 of BLIP	Ser 106, Pro 107, Val108	Zhang et al.,2004..
Loop 2 of BLIP	Interacts with 99QNDLV103 of TEM	Zhang et al.,2004.

The interacting residues on TEM-1 β-lactamase and BLIP are listed in Table 1.2. Two loops on BLIP (loop 1, residues 46-51; loop 2, residues 136-144) insert into the active site of TEM-1 β-lactamase (Strynadka et al., 1992). Asp49 forms two salt bridges and two hydrogen bonds with four conserved TEM-1 residues (Ser130, Lys234, Ser235, and Arg244) that are important for enzyme activity within loop 1 (Strynadka et al., 1992). The carboxylate of Asp49 assumes the position of the carboxylate of penicillin G in the acyl-enzyme complex of TEM-1 with penicillin G (Strynadka et al., 1992). Phe142 is responsible for most of the van der Waals interactions in loop 2, and it mimics the benzyl group of penicillin G for binding TEM-1 (Strynadka et al., 1992). Mutation of Asp49 and Phe142 to alanine causes 20-fold decrease in binding affinity for TEM-1 β-lactamase. Other loop residues do not have a major role in binding with the exception of Tyr50. 50-fold and greater increase in binding affinity is caused by mutation of this residue to alanine (Zhang and Palzkill, 2003).

The ability of BLIP to bind to such a variety of class A β-lactamases is believed to be due in part to an extensive layer of water molecules that are trapped between the inhibitor and the 99–112 loop-helix region of the enzyme (Figure 1.3.A). It has been suggested that the critical residues in this region for binding with BLIP are the aromatic residue at position 105 and the preserved proline at position 107 (Figure 1.3.B) (Strynadka et al., 1996).

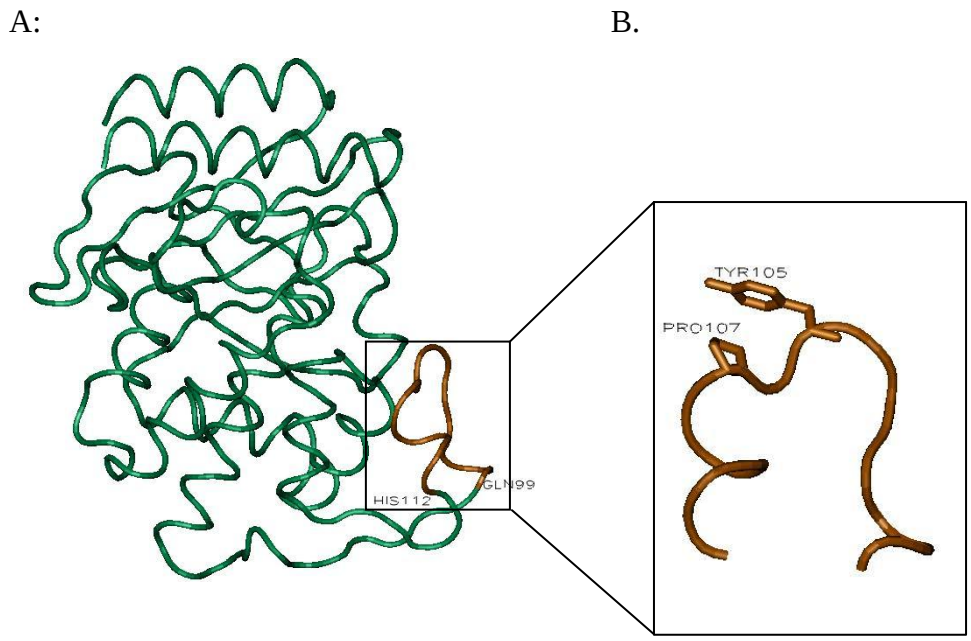

Figure 1.3. A. Representation of TEM-1 (green) the region of BLIP from residues 99 to112 is shown in orange. B. Enlarged representation of the 99-112 loop of TEM-1 β-lactamase (pdb code: 1ZG4)

The three-dimensional structures of BLIP alone and BLIP in complex with the TEM-1 β-lactamase have been determined to high resolution and the structure of the complex indicates that a type II' β turn encompassing residues 46 to 51 of BLIP (Figure 1.3.A) makes critical interactions with the active site of the TEM-1 β-lactamase. Because of these interactions, it was hypothesized that a peptide that includes turn residues 47 to 50 would retain sufficient binding energy to interact with β-lactamase in the absence of the remaining portion of BLIP. If this peptide binds and inhibits β-lactamase, it can serve as a starting point for the design of peptide analogues that inhibit β-lactamase (Rudgers et al., 2001).

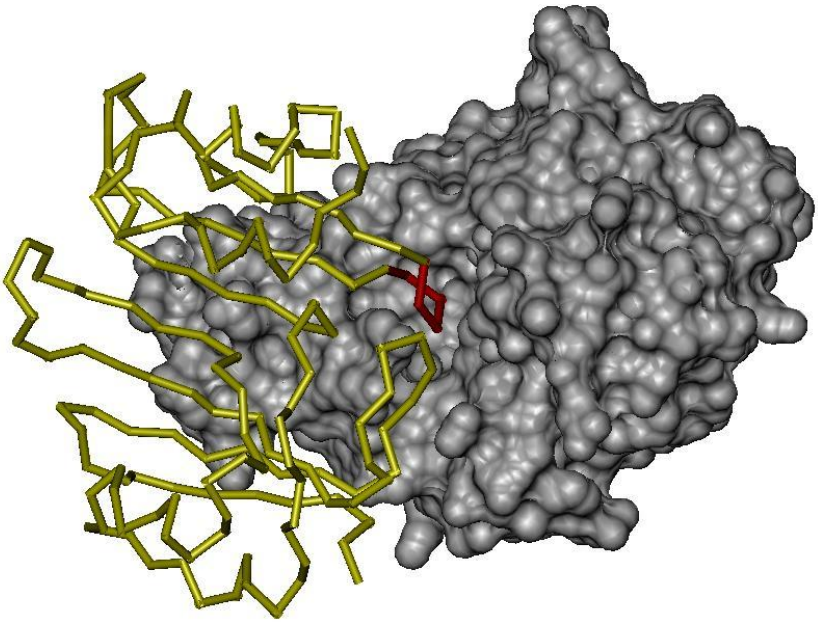

Figure 1.4. Representation of BLIP (yellow) binding to TEM-1 β-lactamase (white, surface model). The region of BLIP from residues 46 to 51 is shown in red (pdb code:1JTG).

1.2. Recent Research on TEM-1 β-lactamase Ligand Recognition

Recent molecular dynamics applications on β-lactamases focus on TEM-1 β-lactamase ligand recognition (Diaz et al, 2003, Roccatano et al., 2005, Joughin et al., 2005). A 5ns molecular dynamics simulation study of TEM-1 β-lactamase (Roccatano et al., 2005), showed that that the dynamical behaviour is characterized by a closure motion around an axis passing near the two hinge regions and the omega loop, forming one edge of the catalytic region (Roccatano et al., 2005).

Binding studies were conducted using immobilized BLIP and inhibition experiments have been conducted *in vitro* by direct application of BLIP to purified enzyme. The 3-dimensional structure of BLIP in complex with TEM-1 β-lactamase shows that the β-turn encompassing residues 46 to 51 of BLIP (Figure 1.4.) make critical interactions with the enzyme (Strynadka et al., 1996). In view of this observation short peptides containing only residues between 40-50 were tested for binding and inhibition. Binding experiments were conducted using synthesized peptides linked to biotin and the BLIP peptides without the N-terminal biotin were tested for inhibition of TEM-1 β-lactamase in solution by

quantitative assay methods (Rudgers et al., 2001). The results showed binding which were approximately 106 fold weaker than the binding by wild type BLIP. In another study (Huang et al., 2003) a combination of phage display and SPOT synthesis were used to identify and optimize peptides that bind and inhibit TEM-1 β-lactamase. A linear 6 mer peptide with the sequence RRGHYY was found to inhibit TEM-1 β-lactamase with a K_i of 136 μM. Using yeast two-hybrid system (Sun et al., 2005) peptides with the ability to bind β-lactamase *in vivo* were found. In this study random oligonucleotide fragments containing the amino acid sequence AAGDYY were fused with the activating domain of p GAD424 and a DNA fragment encoding β-lactamase was fused with the binding domain of pGBT9(+2). The interaction of the peptides and β-lactamase were induced by X-gal or ONPG and two positive clones were obtained. In the inhibition assay *in vitro* of one the binding peptide was found to be inhibitory though no inhibition constant was reported.

In another study (Selzer et al., 2000) a computer algorithm was used to design BLIP mutants with enhanced binding affinities (around 250 fold compared to wild type) for β-lactamase. Experimental measurements using stopped-flow fluorescence and surface plasmon resonance were used to validate predicted enhancements in the binding affinities. *In vitro* inhibition studies showed that within the initial 50s of the experiment the inhibition of TEM-1 by wild type BLIP was negligible, for 2 mutants full inhibition of TEM 1 was observed almost instantantenously.

1.3. Objectives and Plan of the Study

The main objective of this study is to gain a better understanding of the interaction between β-lactamases and the β-lactamase inhibitory protein (BLIP) in order to design novel inhibitory proteins which effectively counter the deleterious effects of β-lactamases. In order to elucidate the binding properties of TEM-1, molecular dynamics simulations of TEM-1 in the presence of BLIP and BLIP based peptides were performed. Mutation of one important BLIP residue (Asp49) on BLIP and the BLIP based peptide resulted in less favorable binding free energy values as well as conformational changes in TEM-1 – ligand interface. In addition, simultaneous expression of β-lactamase and BLIP in *E.coli* was used to show *in vivo* binding of BLIP to β-lactamase.

2. COMPUTATIONAL METHODS

2.1. Simulation Systems

The 3-dimensional X-ray structures are available for TEM-1 (pdb code:1zg4) and TEM-1·BLIP complex (pdb code:1jtg). BLIP was also extracted from this complex. These structures were used as the initial coordinates for the simulations.

One of the peptides used in this simulations is composed of residues 45 to 51 of BLIP ;COO-HAAGDYYA-NH2 since it has been shown that residues 46 to 51 of BLIP make critical interactions with the active site of the TEM-1 β-lactamase (Rudgers et al., 2001). Another peptide is the same peptide with a mutation on Asp49; COO-HAAGAYYA-NH2 (Figure 2.1). Last peptide is designed as residues 142 to 152 of BLIP (FYRGSAHLWFY) (Figure 2.2) since its 142, 148 and 150 residues of BLIP are located in the BLIP's functional epitope and play a significant role for the inhibition of TEM-1 β-lactamase.

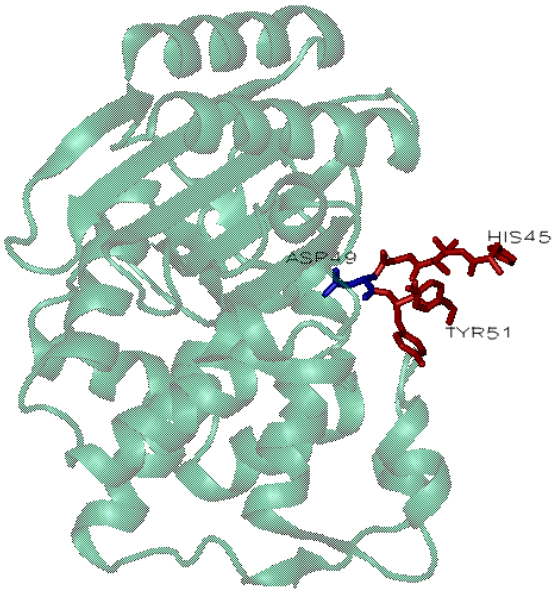

Figure 2.1. Structure of the TEM-1 β-lactamase (green) - HAAGDYYA peptide (red) complex. Asp49 residue on the peptide (blue) is mutated to alanine in mutant peptide.

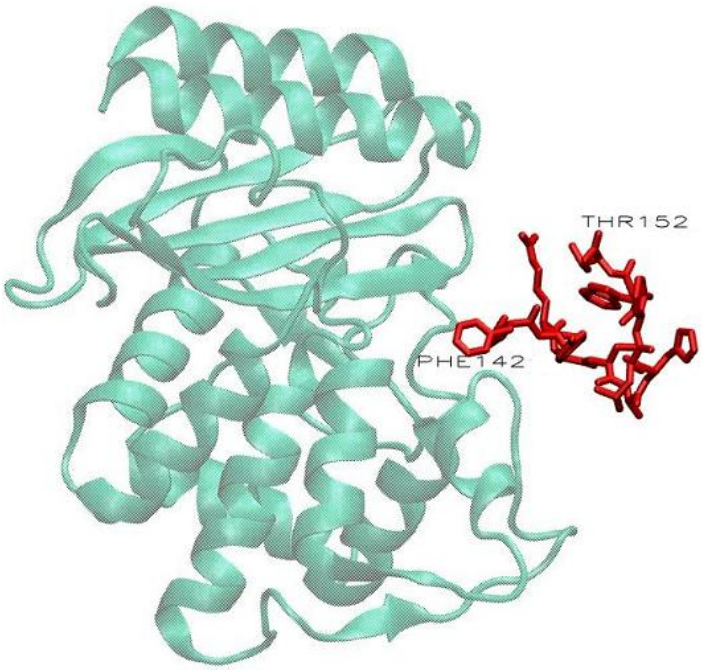

Figure 2.2. Structure of the TEM-1 β-lactamase (green)- FYRGSAHLWFY peptide (red) complex.

2.2. Molecular Dynamics Simulations

Molecular dynamics simulations are used to calculate atomic trajectories by direct integration of the equations of motion. Newton's second law (Equation.2.1) for classical particles with appropriate specification of an inter-atomic potential and suitable initial and boundary conditions

$$F_i = m_i a_i \quad \text{or} \quad \frac{F_i}{m_i} = \frac{d^2 x_i}{dt^2} \tag{2.1}$$

where F_i is the force exerted on the particle i, m_i is its mass and a_i is its acceleration.

Simulations can provide the atomistic detail concerning individual particle motions as a function of time. Thus, they can be used to address specific questions about the properties of a model system, sometimes more easily than experiments on the actual

system. For many aspects of biomolecular function, it is these details that are of interest. Experiments play an essential role in validating the simulation methodology: comparisons of simulation and experimental data serve to check the accuracy of the calculated results and to provide criteria for improving the methodology.

Another significant aspect of simulations is that, although the potentials used in simulations are approximate, user has control over the potential, so that by removing or altering specific contributions, the role of a particular interaction or energy in determining a given property can be examined. This is most graphically demonstrated by the use of "computer alchemy" in the calculation of free energy differences, such as that used in computational alanine scanning (Karplus and McCommon, 2002).

2.2.1. Force Field

The application of mathematical equations to describe the relationship of chemical structure to energy in combination with statistical mechanics, allows for all properties of a system to be calculated in theoretical chemistry. However, this is limited by the inability to calculate the energy of all possible conformations of a chemical system. One way to overcome this limitation is the use of simple mathematical functions to treat the structure-energy relationship. This type of approach is referred to as molecular mechanics or empirical force field calculations. However, the equation alone does not allow for computation of structure-energy relationships. In addition, parameters must be included in the mathematical equation. The empirical force field used in this study is CHARMM22 (MacKerell, Parameter Notes).

Intramolecular

$$\sum_{bonds} K_b (b - b_o)^2 + \sum_{angles} K_\theta (\theta - \theta_o)^2 + \sum_{torsions} K\phi(1+\cos(n\phi - \delta)) + \tag{2.2}$$

$$\sum_{impropers} K_\varphi (\varphi - \varphi_o)^2 + \sum_{Urey-Bradley} K_{UB}(r_{1,3} - r_{1,3,o})^2$$

Intermolecular

$$\sum_{electrostatics} \frac{q_i q_j}{r_{ij}} + \sum_{VDW} \left[\left(\frac{R_{\min ij}}{r_{ij}} \right)^{12} - 2 \left(\frac{R_{\min ij}}{r_{ij}} \right)^{6} \right] \tag{2.3}$$

The first term in the energy function (Equation 2.2) accounts for the covalent bond strecthing interaction between two atoms linked by a harmonic potential where b_0 is the minimum energy bond length, hence b-b_0 is the distance from equilibrium that the atom has moved and K_b is the bond force constant. The second term in the equation accounts for the bond angles where K_0 is the angle force constant and θ-θ_0 is the angle from equilibrium between 3 bonded atoms. The third term is used for the dihedral angle interaction where $K\varphi$ is the dihedral force constant, n is the multiplicity of the function, φ is the dihedral angle and δ is the phase shift. The fourth term accounts for the impropers, where k_w is the force constant and w-w_0 is the out of plane angle. The Urey-Bradley component (cross-term accounting for angle bending using 1,3 nonbonded interactions) comprises the fifth term, where k_u is the respective force constant and U is the distance between the 1,3 atoms in the harmonic potential. Nonbonded interactions between pairs of atoms *(i,j)* are represented by the last two terms. By definition, the nonbonded forces are only applied to atom pairs separated by at least three bonds. The van der Waals (VDW) energy is calculated with a standard 12-6 Lennard-Jones potential and the electrostatic energy with a Coulombic potential. In the Lennard-Jones potential above, the $Rmin_{ij}$ term is not the minimum of the potential, but rather where the Lennard-Jones potential crosses the x-axis (*i.e.* where the Lennard-Jones potential is zero). Non-bonded forces decrease as the distance between atoms increases. Many simulations use a cutoff radius to save computation time (Kalé et al., 1999; Baker and McCammon, 2003).

2.2.2. NAMD

NAMD2 (Kalé et al., 1999), is one of the new parallel programs aimed at utilizing large parallel machines in a scalable manner. The non-bonded force computations, which constitute the dominant component of the overall computational cost, require calculation of pairwise interactions between atoms. In most common methods, a cutoff distance is used.

Non-bonded interactions between atoms beyond this cutoff radius are either not calculated or calculated less often.

NAMD2 allows the force field to be divided into three parts based on their variation frequency. All bonded forces (bonds, angles, dihedrals, and impropers) are considered quickly varying, non-bonded forces (electrostatics and Lennard-Jones) within a cutoff are slower, and long-range electrostatics vary on the slowest time scale.

NAMD2 is written using Charm++, a parallel C++ extension that supports message-driven execution. NAMD2 uses CHARMM force fields and X-PLOR coordinate and molecular structure files. In addition to non-periodic simulations, NAMD2 can use periodic boundary conditions over any combination of the three coordinate axes. It performs cutoff simulations or full-electrostatic simulations. NAMD2 can connect to VMD (Humphrey et al., 1996), allow monitoring of and interaction with ongoing simulations (Kalé et al., 1999).

2.2.3. Simulation Parameters

The initial coordinates for the protein atoms and the crystallographic water molecules were obtained from the crystal structure of the TEM-1 β-lactamase at 1.55 Å resolution and TEM-1·BLIP complex structure at 1.73 Å resolution. (PDB ID code: 1zg4 and 1jtg, respectively). The MD simulations were performed with the NAMD program using the CHARMM force field. To generate the models the protein was surrounded by a periodic box of TIP3P water molecules. The SHAKE algorithm was applied to constrain all bonds including hydrogen atoms within their equilibrium values. Particle Mesh Ewald method was used for long range electrostatic interactions. Particle Mesh Ewald (PME) divides the electrostatic potential into a local interaction which must be calculated within a cutoff, and a smooth, long-range interaction which is evaluated on a grid via a three dimensional fast Fourier transform. After the whole simulation system was energy minimized 3000 steps, the system was gradually heated up to the simulation temperature of 300K in 8 ps. Total simulation length was 10 ns.

2.3. Trajectory Analysis

2.3.1. Root Mean Square Deviations

Calculation of the root-mean square distance between equivalent atoms of the two superposed structures is the most popular method for measuring structural similarity. The root mean square deviations are calculated as the deviations from the initial structure of the coordinates throughout MD simulations (Equation 2.4). d_i; distance between the atom coordinates, i; RMSD'si, N is the number of atoms.

$$rmsd = \frac{\sqrt{\sum_{i=1}^{N}(d_i^2)}}{N} \tag{2.4}$$

2.3.2. Mean Square Fluctuations of Positions

The mean square fluctuations are calculated as the deviation from the avarage structure, avareged through the whole trajectory of the simulations (Equation 2.1). The conformations are aligned before calculation of flactuations.

$$\Delta R_i = \langle R_i(t) - R_i^0 \rangle \tag{2.5}$$

2.3.3. PCA Analysis

Principal components analysis is used to reduce large dimensional data sets to data sets with a few dimensions which still retain most of the information in the original data matrix.

Given a data matrix X with n cases and p variables (i.e., $X_1, X_2 ..., X_p$ variables) a linear transformation to a new set of variables $Y_1, Y_2 ..., Y_p$ can be calculated with Equation 2.6, Equaion 2.7, and Equation 2.8) :

$$Y_1 = a_{11}X_1 + a_{21}X_2 + ... + a_{p1}X_p \quad (2.6)$$

$$Y_2 = a2X_1 + a_{22}X_2 + ... + a2X_p \quad (2.7)$$

...

$$Yp = apX_1 + apX_2 + ... + apX_p \quad (2.8)$$

The first principal component explains the largest percentage of the variation in the original p-dimensional data set (and the second principal component explains the second largest percentage and so on). Typically the first few principal components account for most of the variation while the remaining principal components make a negligible contribution. By reducing the dimensionality of the original data, principal components can often simplify many analyses.

Principal components reduce to the problem of finding the eigenvalues and eigenvectors of the covariance (or correlation matrix) of the data matrix. The *i*th row of the A matrix is the eigenvector corresponding to the *i*th eigenvalue of the covariance (or correlation) matrix. Also, the proportion of the variance in the original data matrix explained by the *i*th principal component is the *i*th eigenvalue divided by the sum of all p eigenvalues. Covariance matrix is preferred when the original data have reasonably comparable scales. If this is not the case, the correlation matrix is preferred.

2.4. Binding Fee Energy Calculations

2.4.1. Molecular Mechanics Poisson Bolztmann Surface Area (MMPBSA)

MM-PBSA method is a straightforward approach to calculate free energies of macromolecules (Jayaram et al., 1998; Vorobjev et al., 1998, Kollman et al.,2003).

MMPBSA can also be applied computational mutagenesis to estimate the free energies for ligand binding to proteins (Laitinen et al., 2003).

After running molecular dynamics simulation of the complex in a periodic water box with counterions, the resulting trajectory is post processed by removing the solvent and the periodicity (Page and Bates, 2006). In the MM/PBSA approach, It is more important to pay attention to adjusting model parameters such as atomic radii and solute di-electric constant rather than looking for more physical (and complex) implicit solvent representations in order to reproduce experimental observations (Fogolari et al., 2003). Average binding free energy (ΔG_{bind}) is computed as a sum of (Equation 2.9) gas phase energies (ΔE_{MM}), solvation free energies ($\Delta\Delta G_{solv}$) and entropy contributions ($-T\Delta S$) which are averaged over snapshots extracted from MD trajectories (Laitinen et al., 2006).

$$\Delta G_{bind} = \Delta E_{MM} + \Delta\Delta G_{solv} - T\Delta S \qquad (2.9)$$

This approach has been used to compare relative stabilities of different conformations of nucleic acids (Srinivasan et al., 1998), to identify correctly folded proteins (Lee et al., 2001), and to estimate binding affinites of small molecules binding to proteins(Kuhn and Kollman, 2000; Lee Kollman, 2000; Wang et al.,2001). It has been used to predict the effects of amino acid mutations on binding affinities (Gohlke et al., 2003). Kollman and coworkers who analyzed explicit solvent MD trajectories using the MM/PBSA approach and used the free energy thus computed to discriminate between native and nonnative like conformations for two small peptides in one of the application of this methodology (Kollman et al., 2000; Lee et al., 2001).

The MMPBSA method is somewhat less accurate but a substantially faster approach compared to the more traditional free energy perturbation simulations (Kuhn and Kollman, 2000). In addition, the MMPBSA method can be applied to systems not suitable for free energy perturbation calculations (Laitinen et al., 2003). When parameters are properly chosen, the MMPBSA approach affords an accuracy comparable or superior to explicit solvent simulation methods (Fogolari et al., 2003).

3. COMPUTATIONAL RESULTS

Six different trajectories in the presence and absence of ligand were calculated to study the binding and dynamics of TEM-1 – ligand recognition (Table 1). In addition, five simulations on the free ligand were calculated to characterize the properties of the ligands in the apo form (Table 2). Geometric and energetic analyses were performed on the trajectories.

3.1. Root Mean Square Deviations from Initial Structure

Root mean square deviation (RMSD) of a conformation was calculated by aligning its alpha-carbon backbone to the initial structure of MD simulation and then calculating the deviation of each atom from its initial position as averaged over all atoms.

RMSD values give an idea about the equilibration period of the simulations and also show the motions of the proteins throughout the simulation.

Table 3.1. RMSD values of TEM-1 beta lactamase with respect to the initial conformation

Simulation	Simulation Length	RMSD(Å)
TEM-1	10ns	0.9
TEM-1·- BLIP	10ns	0.89
TEM-1 - BLIP (D49A)	10ns	0.95
TEM-1 - Peptide(45to52 of BLIP)	10ns	0.95
TEM-1·- Peptide (45to52 of BLIP, D49A)	10ns	1.04
TEM-1·- Peptide (142to152 of BLIP)	10ns	0.97

Table 3.2. RMSD values of BLIP or peptides with respect to the initial conformation

Simulation	Simulation Length	RMSD (Å)
BLIP	10ns	0.94
Mutant BLIP (D49A)	10ns	1.07
Peptide (45to52 of BLIP)	10ns	1.26
Mutant Peptide (45to52 of BLIP,D49A)	10ns	1.69
Peptide (142to152 of BLIP)	10ns	4.05

3.1.1. Tem-1 β-lactamase

The unbound TEM-1 β-lactamase has an RMSD of 0.9 Å at the end of the 10ns simulation (Figure 3.1). There are no significant fluctuations in RMSD. The system reaches equilibrium after about 1.5 ns.

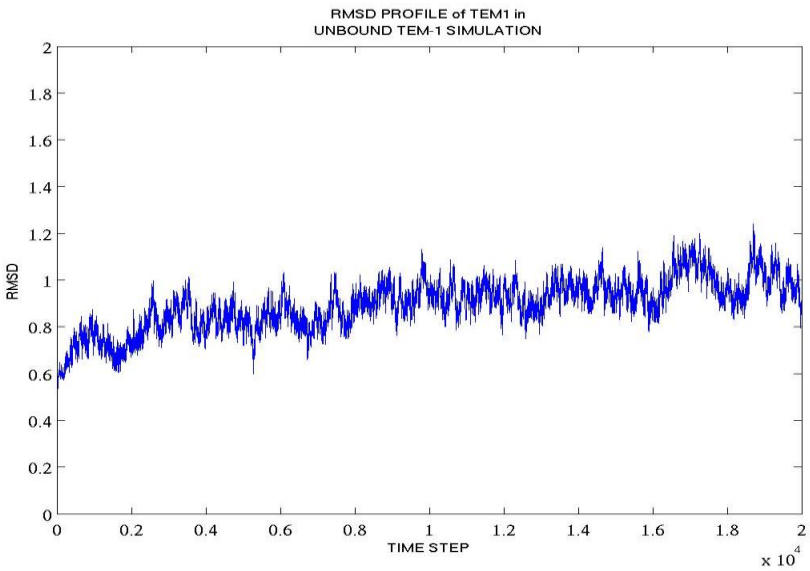

Figure 3.1. Root Mean Square Deviation of Apo TEM-1 β-lactamase

The TEM-1 – BLIP complex and TEM-1 – BLIP (D49A) complex simulations were calculated for 10ns. The RMSD profiles (Figure 3.2) show that RMSD values reach

equilibrium after about 3ns at 0.88 Å and 0.95Å, respectively. They reveal a stable behaviour with low amplitude fluctuations during the time course of the simulation.

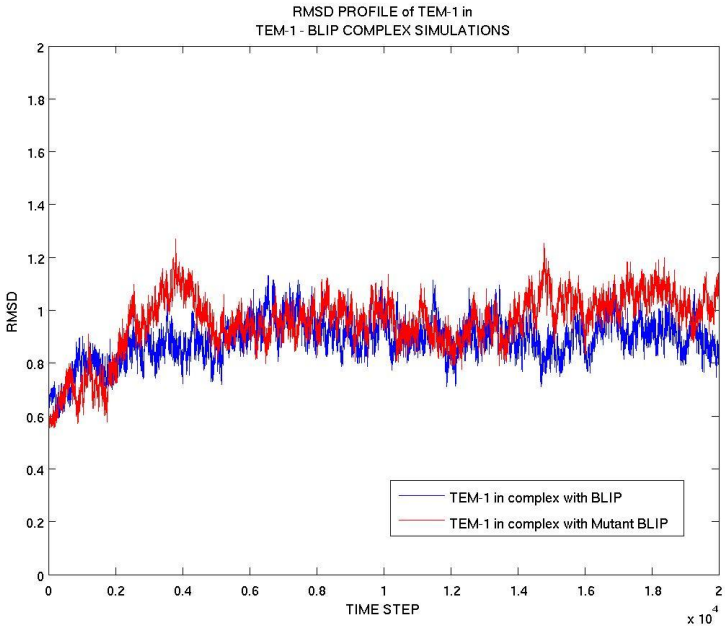

Figure 3.2. RMSD of TEM-1 β-lactamase in TEM-1 – BLIP (blue) and TEM-1 – BLIP (D49A) complex (red).

The RMSD of TEM-1 β-lactamase in TEM-1 - peptide complex simulations is given in Figure 3.3. Peptides derived from residues 45 to 52 of BLIP (HAAGDYYA) , 45 to 52 of BLIP with a mutation (HAAGAYYA) and residues 142 to 152 (FYRGSAHLWFY) of BLIP are shown in blue, pink and black, respectively. TEM-1 β-lactamase reached equilibrium in all three cases. The average RMSD values are 0.95, 1.04, 0.97 for TEM-1 – peptide complexes in which the peptides were residues 45 to 52 of BLIP, residues 45 to 52 of BLIP (D49A), and residues 142 to 152 of BLIP.

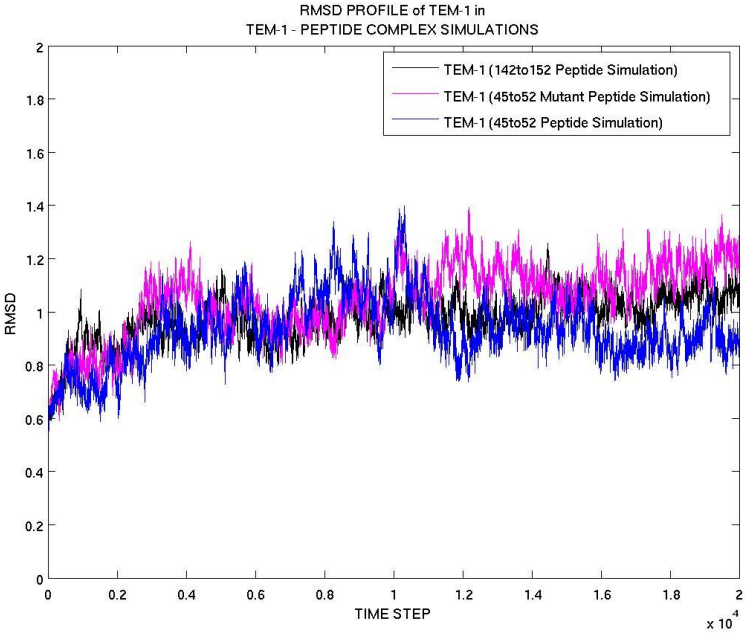

Figure 3.3. RMSD of the carbon-α atoms of TEM-1 β-lactamase complexes with peptides.

3.1.2. β-lactamase Inhibitory Protein

The RMSD profiles of the substrates were calculated. Substrates were either BLIP or peptides derived from BLIP. The RMSD values are calculated by first superpositioning the substrate structures on the initial structure of the substrate. RMSD values report changes in the internal structure of the substrate.The purpose of measuring substrate deviations is to elucidate the changes in the dynamic properties of the substrates upon binding.

The individual RMSD values of BLIP and mutant BLIP fluctuate around 1 Å Figure 3.4). The maximum RMSD value observed during the simulations is around 1.4 Å. The RMSD of BLIP for 10 ns in TEM-1-BLIP, TEM-1 – mutant BLIP (D49A) complex is given in figure 3.5. The RMSD profile begin to exhibit high fluctuations in the complex form. However, the RMSD profile of the BLIP in the mutant form (D49A) looks like the unbound in terms of equilibrium states.

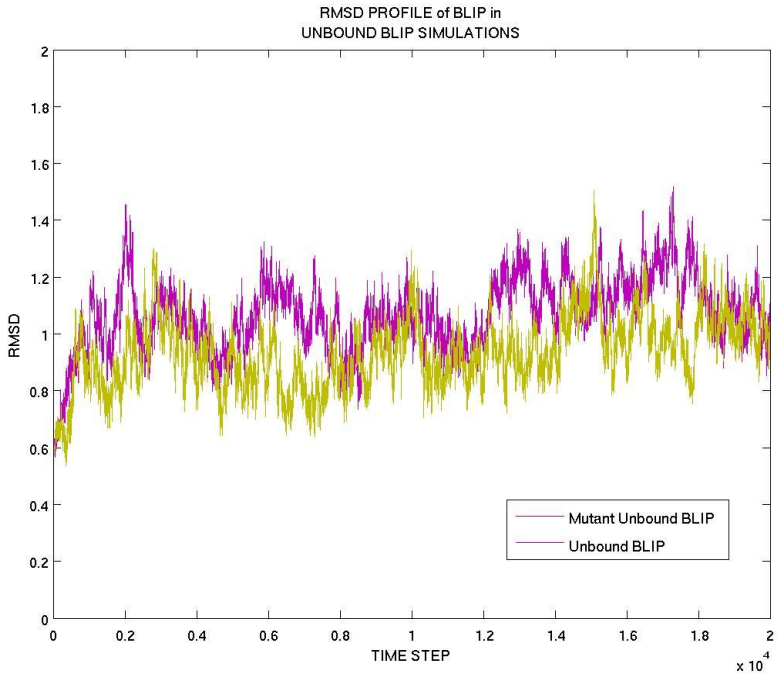

Figure 3.4. BLIP and Mutant BLIP RMSD from the intial structure throughout the trajectory.

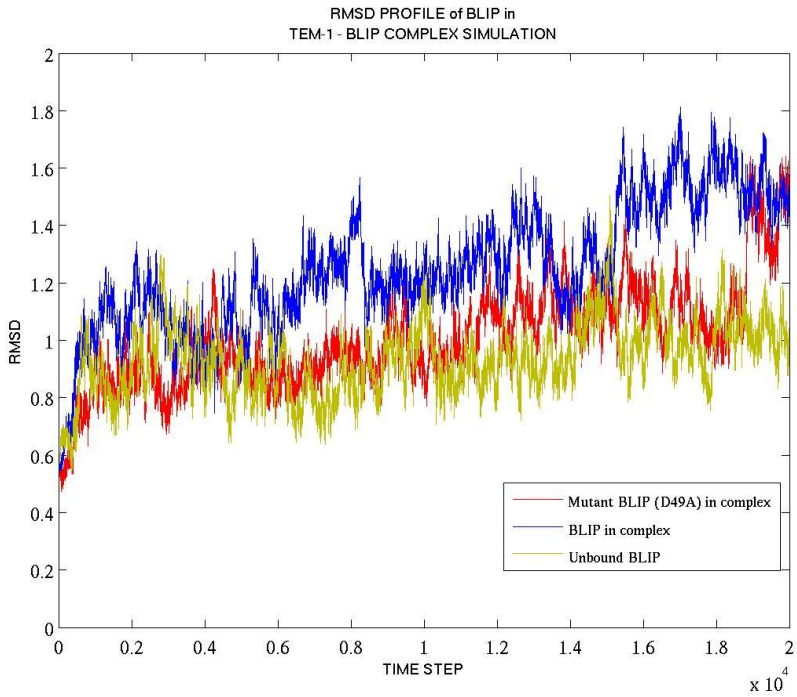

Figure 3.5. RMSD profiles of BLIP with respect to the initial structure throughout the trajectory in apo BLIP, TEM-1 BLIP and TEM-1 - mutant BLIP (D49A) complex

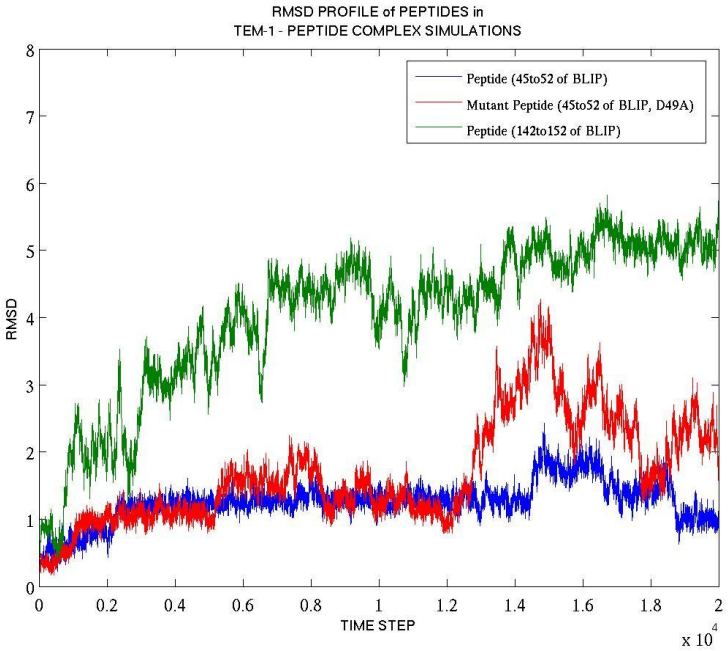

Figure 3.6. RMSD profiles of the peptides with respect to the intial structure throughout the trajectory.

Simulations on the TEM-1 β-lactamase complexed with peptide structures derived from residues 45 to 52 of BLIP (HAAGDYYA) and 45 to 52 of mutant BLIP seem to reach equilibrium in the first six ns, however it exhibits fluctuations afterwards as can be seen in Figure 3.6. In the Figure 3.6 region 45-52 of BLIP, region 45 to 52 of BLIP and region 142 to 152 of BLIP is shown in blue, red and green, respectively. In order to see if the simulation will reach equilibrium the simulation time can be extended. On the other hand, the other peptide which is composed of residues 142 to 152 of BLIP shows higher fluctuations in its RMSD profile. This peptide may have significant conformational changes during simulation.

3.2. Mobility and Flexibility of Structures from MD Simulation Trajectories

3.2.1. Wild type TEM-1 β-lactamase

The mean-square fluctuation of each residue in Tem-1 β-lactamase is calculated within a 10ns time scale. The peaks in the graph show the mobile regions of the structure.

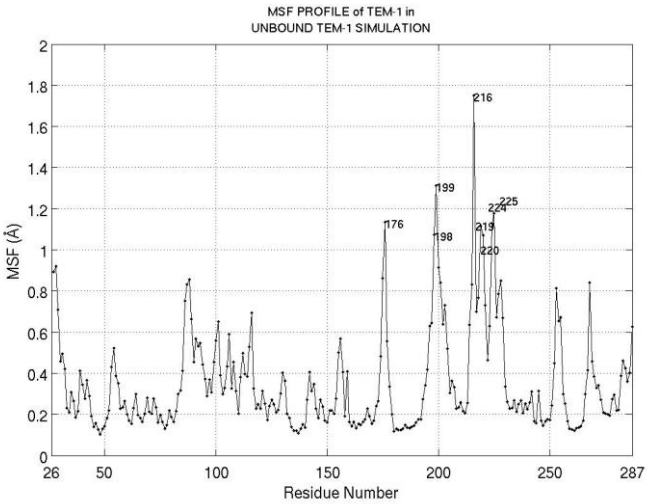

Figure 3.7. Mean square fluctuation of TEM-1 β-lactamase.

In the wild type unbound TEM-1 simulation Tyr 216 residue which is on the loop region of TEM-1 shows the highest fluctuation.

A. B.

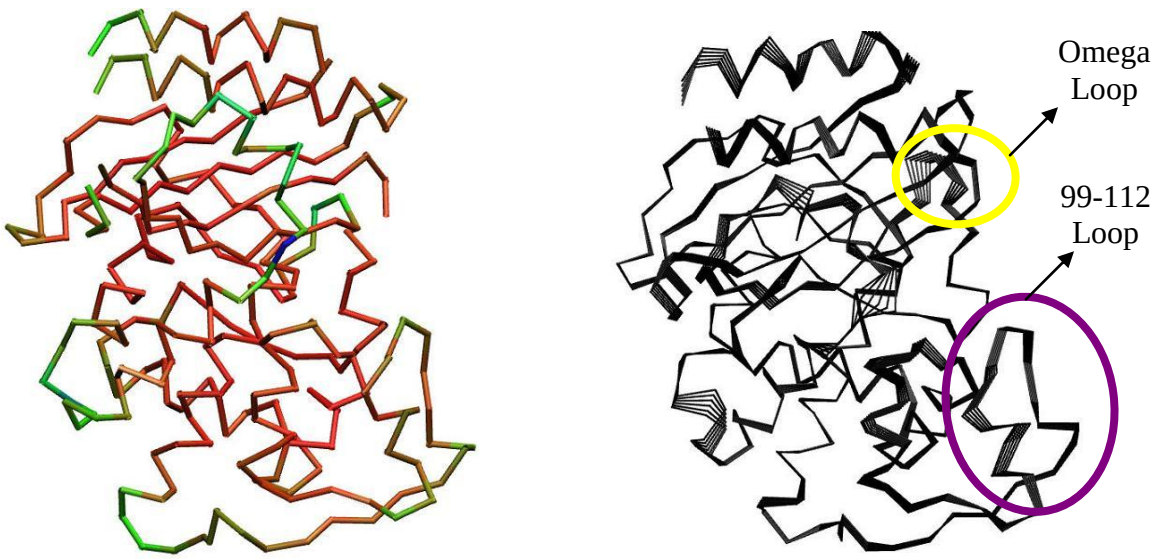

Figure 3.8. A. TEM-1 β-lactamase colored according to mobility color scheme. B. Principal component analysis of TEM-1 β-lactamase.

Mobility of TEM-1 β-lactamase for the unbound enzyme can be seen in Figure 3.8.A and 3.8.B. In Figure 3.8.A red regions are the most rigid structures during the simulation, blue shows more mobile region than red ones and the green indicate the most flexible residues.

In Figure 3.B snapshots were taken from the first principal component analysis of CA trajectory of TEM-1 β-lactamase for the unbound enzyme

Recent studies indicates that over two thirds of all contacts made by BLIP are with the 99-112 loop-helix of TEM-1 β-lactamase (Strynadka et al.,1996). 99-112 loop-helix of the enzyme (circled with black color on Figure 3.8.B.) maintained its structure during 10ns MD simulation (Figure 3.7). H10 helix is stable however one edge of the omega loop (172-176,yellow circled) is the most flexible region in Tem-1 β-lactamase.

3.2.2. TEM-1 – BLIP Complex

The values for the fluctuations are calculated by aligning each part of the complex on its own structure.

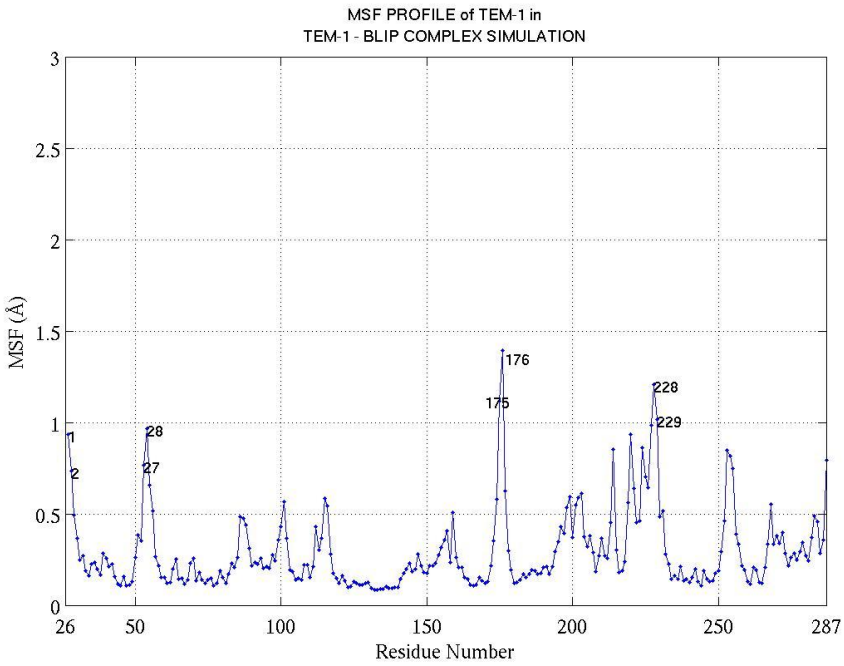

Figure 3.9. Mean square fluctuation of TEM-1 β-lactamase in TEM-1 - BLIP complex.

A. B.

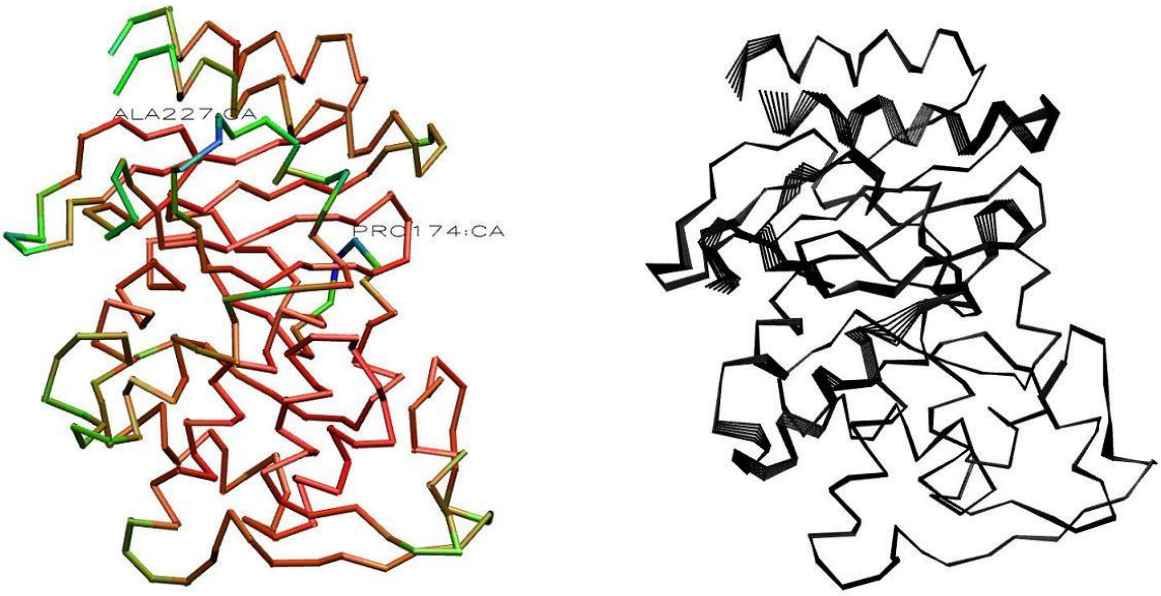

Figure 3.10. TEM-1 β-lactamase in TEM-1 - BLIP complex simulation. A. TEM-1 β-lactamase structure colored according to the MSF values B. PCA of TEM-1 β-lactamase

In Figure 3.10.A TEM-1 β- lactamase mobility is shown and the principal component analysis of trajectory of TEM-1 β- lactamase for the TEM-1 – BLIP complex can be seen in Figure 3.10.B. The color scale is the same as that of Figure 3.8.

3.2.3. TEM-1 – Mutant BLIP Complex

Comparison of the residue based MSF plots for the simulations on the TEM-1 – BLIP complex with that on the TEM1 – BLIP (D49A) complex show that the residue Tyr176 which is located in the Ω loop, forming one edge of the catalytic region, is to be more mobile upon formation of the complex with β-lactamase inhibitory protein with a mutation on Asp49 (see Figure 3.11 and Figure 3.12.A).

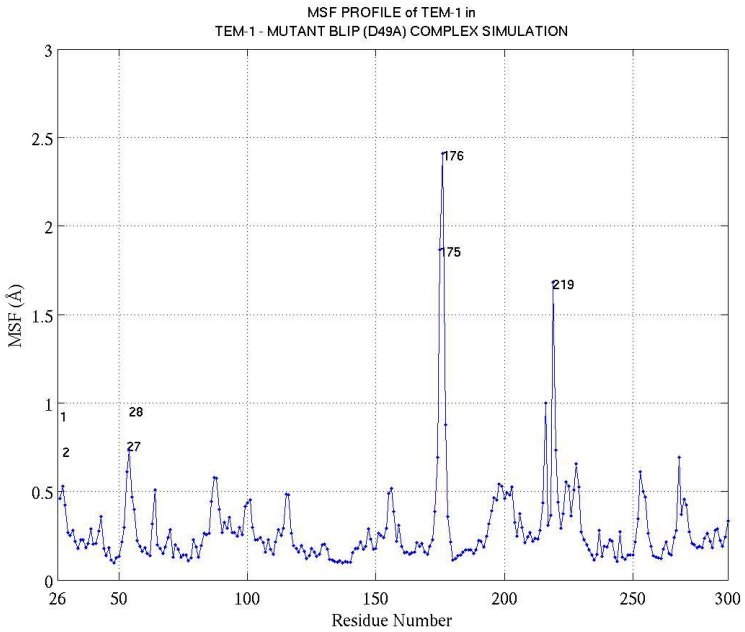

Figure 3.11. Mean square fluctuation of TEM-1 β-lactamase in TEM-1 – mutant BLIP (D49A) simulation.

A. B.

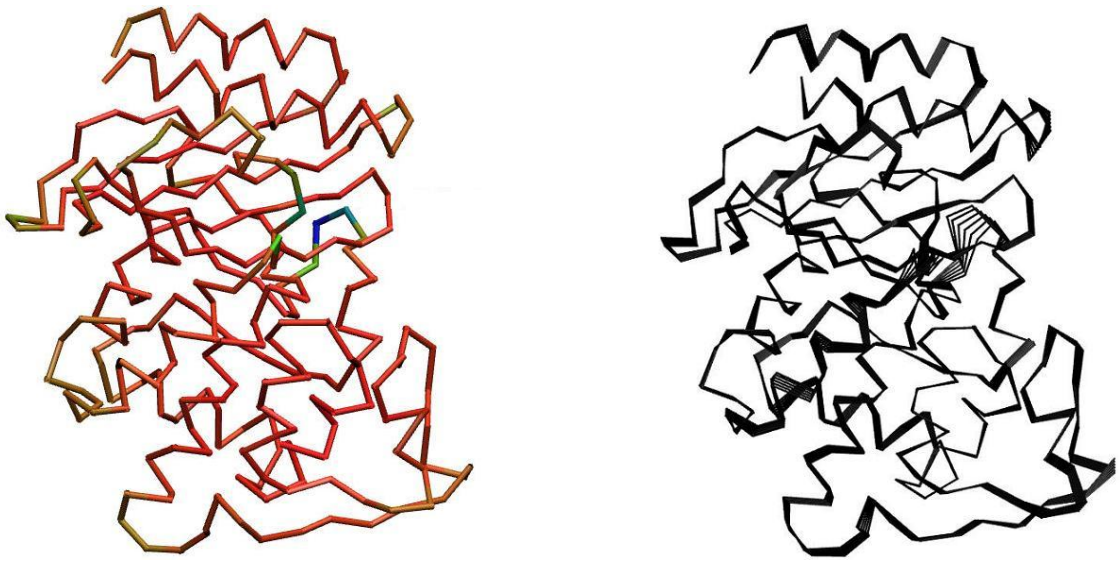

Figure 3.12. Mobility of TEM-1 β-lactamase in TEM-1 - BLIP (D49A) complex A. TEM-1 β- lactamase structure B. PCA of the TEM-1- mutant BLIP (D49A) complex

In Figure 3.12.B projection along the first principal component (eigenvector) of the TEM-1- mutant BLIP (D49A) complex MD trajectory reveals regions of high variance. The color scale of Figure 3.12 is the same as that of Figure 3.8.

3.2.4. TEM-1 – Peptide Complexes

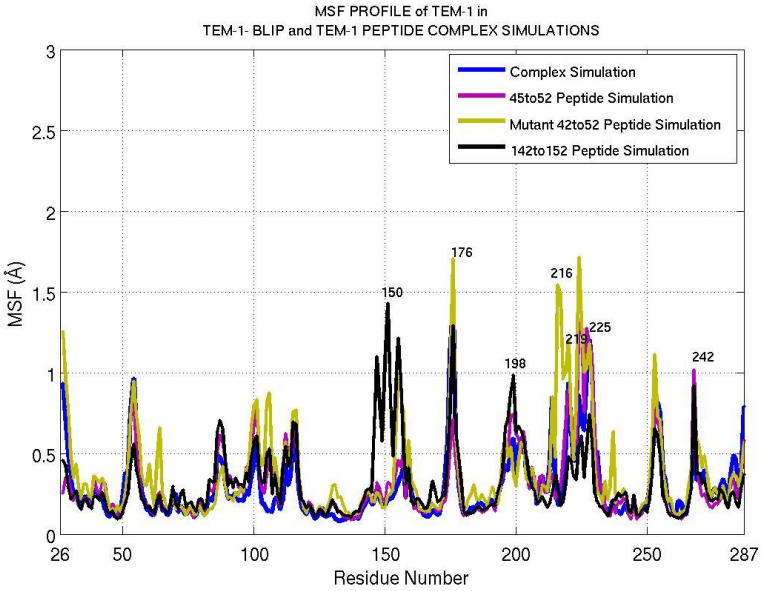

Figure 3.13. Mean square fluctuation of TEM-1 β-lactamase in TEM-1 - peptide complex simulations

It has been shown that Tyr 50 of BLIP has van der Waals interactions with Val 216 residue (Zhang et al., 2003). In Figure 3.13 it can be seen that TEM-1 β-lactamase of 45 to 52 of mutant BLIP peptide (D49A) has a large fluctuation on the 216 residue which means this residue has a large flexibility in this simulation. According to the Figure 3.13, it can be said that the mutation of Asp49 of BLIP effects the interaction between Tyr50 and Val216 and enhanced the mobility of Val216.

Mobility of TEM-1 β-lactamase in TEM-1 – Peptide 1 (45 to 52 of BLIP) complex, TEM-1 – mutant Peptide1 (45 to 52 of BLIP, D49A) complex and TEM-1 – Peptide 2 (45 to 52 of BLIP,D49A) complex are given in Figure 3.14.A, 3.15.A and 3.16.A. The comparison between the peptide 1 and mutant peptide 1 indicates the flexibility of Val 216 residue. While, in the Figure 3.14.A, Val 216 is located in the red regions, which represent the rigid regions, of TEM-1 β-lactamase, in Figure 3.15.A it is located in the blue region, which represent the most flexible regions.

Projection along the first principal component (eigenvector) of the complexes are also examined and Val 216 flexibility was also observed in these analysis. (see Figure 3.14.B, 3.15.B and 3.16.B).

A. B.

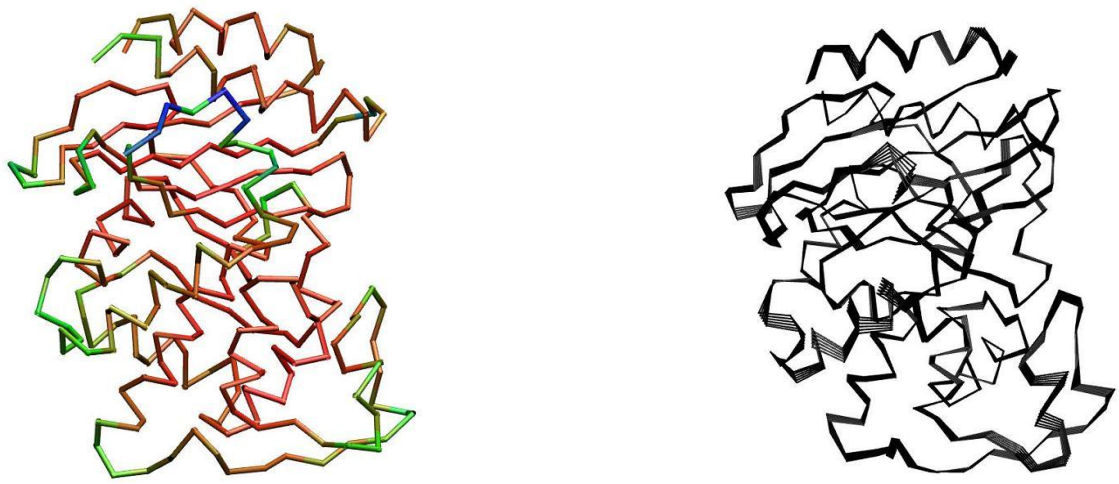

Figure 3.14. Mobility of TEM-1 β-lactamase in TEM-1 – Peptide (45 to 52 of BLIP) complex. A. TEM-1 β- lactamase structure B. PCA of the TEM-1- peptide 1.

A. B.

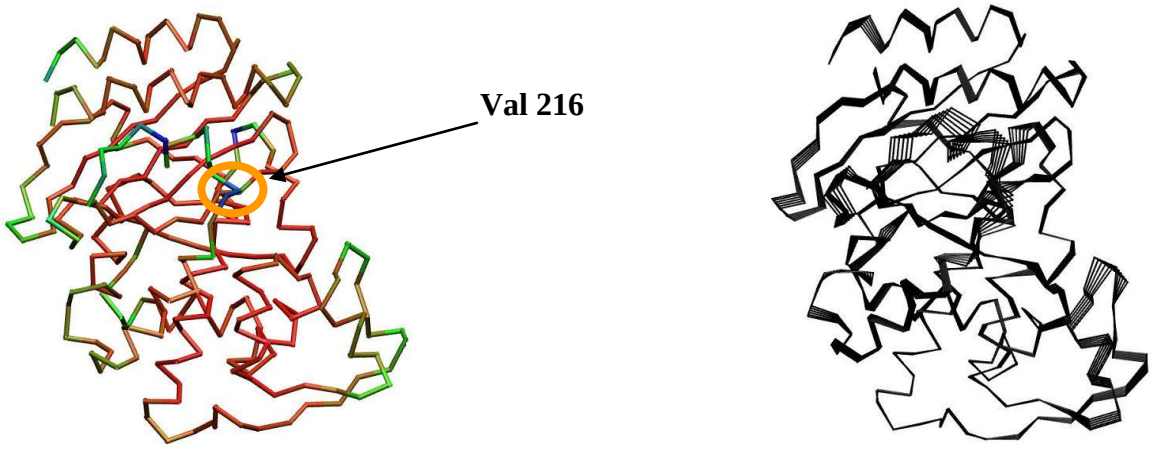

Figure 3.15. Mobility TEM-1 β-lactamase in TEM-1 – Peptide (45 to 52 of BLIP,D49A) complex . A. TEM-1 β-lactamase structure B. PCA of the TEM-1- mutant peptide 1.

A. B.

Figure 3.16. Mobility TEM-1 β-lactamase in TEM-1 – Peptide (142 to 152 of BLIP) complex. A. TEM-1 β-lactamase structure B. PCA of the TEM-1- peptide 2.

3.3. Effect of D49A mutation on BLIP on TEM-1 structure and binding

Crystal structures of BLIP with TEM-1 β-lactamase show that Asp49 of BLIP makes strong hydrogen bond contacts with four conserved residues in the TEM-1 active site pocket: Ser-130, Lys-234, Ser-235, and Arg-244 (17). These residues are conserved in all class A β-lactamases and are involved in the binding and catalysis of β-lactam antibiotics. Mutation of the aspartic acid to alanine removes the carboxylate moiety that serves as a hydrogen bond acceptor for the four active site TEM-1 residues. Elimination of the carboxylate reduces the inhibitory activity of BLIP approximately 100-fold, indicating residue Asp49 makes an important contribution to BLIP inhibition of TEM-1 β- lactamase (Petrosino et al.,1999). Thus, to be able to see the contribution of Asp49 on BLIP to β-lactamase binding, Asp49 was mutated to ALA. The most significant result of this mutation is a check: of interaction with Tyr105 of TEM-1 β-lactamase (Figure 3.17.). In Figure 3.17. TEM-1 – BLIP (D49A) complex and TEM-1 BLIP complex are shown in blue and red, respectively. The closer figure shows the interaction between the 49th residue of BLIP and Tyr105 residue of TEM β-lactamase. 49th residue of BLIP has a closer interaction with 99 -112 loop of TEM-1 as a result of mutation. This behavior results in a loss of interaction between Ala 49 of BLIP and the active site region of TEM-1.

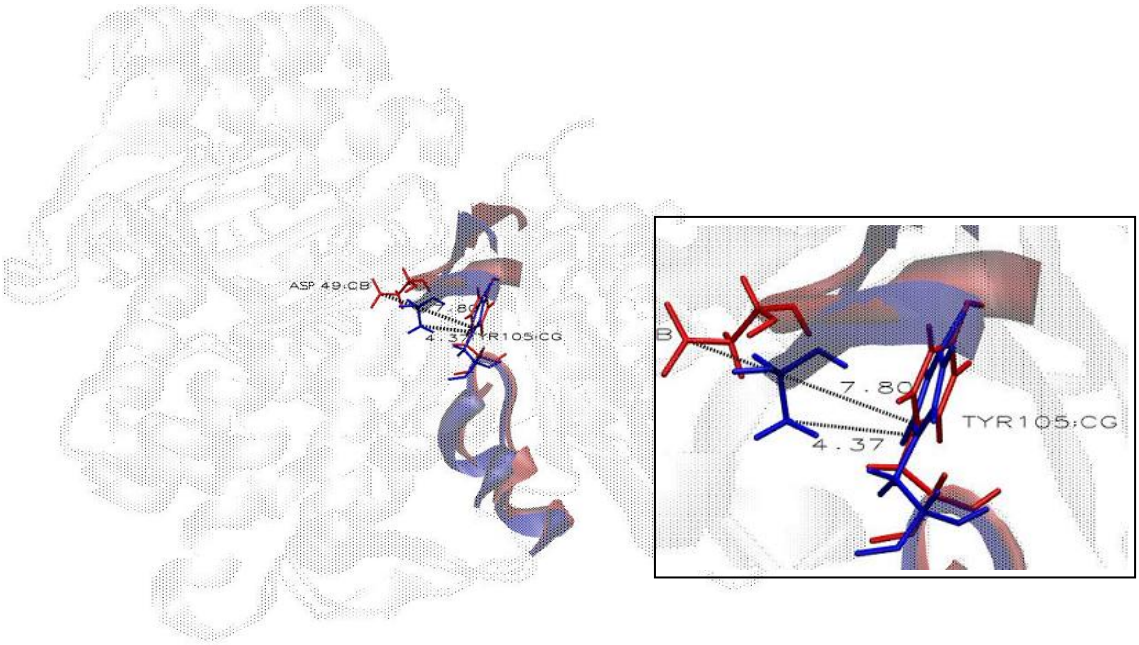

Figure 3.17. Effect of D49A mutation on Tyr 105 TEM-1 β-lactamase residue.

3.4. Important Residue Interactions

Table 3.3. Distances between the active site residues(S70, K73, S130, E166, K234) of TEM-1 β-lactamase (Å). Studied peptide was based on the region 45 to 52 of BLIP. Residue distances were calculated using the terminal heavy atom on the sidechains

RESIDUE	TEM-1	TEM-1 BLIP	TEM-1 BLIP (49A)	TEM-1 Peptide	TEM-1 Peptide(D49A)
S70 – K73	2.70	2.75	**5.06**	2.98	**5.25**
S70 – E166	5.88	3.68	4.98	6.18	7.42
S70 – S130	4.49	3.30	**6.93**	4.15	**5.49**
S70 – K234	2.70	4.00	**7.79**	3.29	**5.99**
K73 – S130	5.39	3.33	3.62	6.09	5.47
K73 – E166	5.41	3.25	4.85	3.53	3.65
K73 – K234	6.93	4.79	5.70	6.12	6.76
S130 – E166	9.02	5.78	8.21	9.49	8.55
S130 – E234	2.65	4.13	2.70	3.07	2.66
E166 – E234	10.02	7.34	9.16	9.45	10.26

3.4.1. Ser 70 – Lys 73

It has been showed that the amine group of Lys 73 can abstract the Ser70 hydroxyl group proton and promote the acylation [Electrostatic analysis of TEM-1]. The distance between the Ser70 and Lys 73 residues of TEM-1 β-lactamase was investigated and significant differences were observed in the distance values at the end of the simulations (Table 3.3).

A. B.

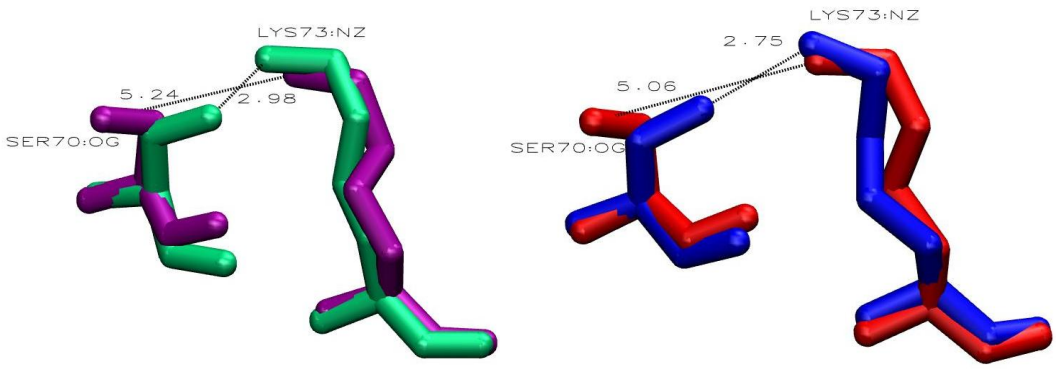

Figure. 3.18. Active site residues of TEM-1 β-lactamase. A. Ser 70 and Lys 73 in TEM-1-peptide simulations. B. Ser 70 and Lys 73 residues in TEM-1 - BLIP simulations.

Figure 3.18 shows the interaction between Serine 70 and Lysine 73 for the simulations of TEM-1 in complex with wild type and mutant substrate. In Figure 3.18.A. Ser 70 and Lys 73 residues of TEM-1 β-lactamase in TEM-1-peptide and TEM-1 mutant peptide (D49A) are shown in green and purple, respectively. In Figure 3.18.B. Ser 70 and Lys 73 residues of TEM-1 β-lactamase in TEM-1 - BLIP and TEM-1 - mutant BLIP (D49A) are shown in blue and red, respectively.

When residue Asp49 of BLIP is mutated to Alanine, the active site residues of Ser70 and Lys73 interaction is also affected by this mutation. The distance between the atoms increases for both BLIP and the BLIP based peptide as a result of the mutation.

3.4.2. Ser 70 – Ser130

The distance between the OG atoms of Ser 70 and Ser130 increases as a result of the mutation on Asp49 in BLIP and in peptide.

A. B.

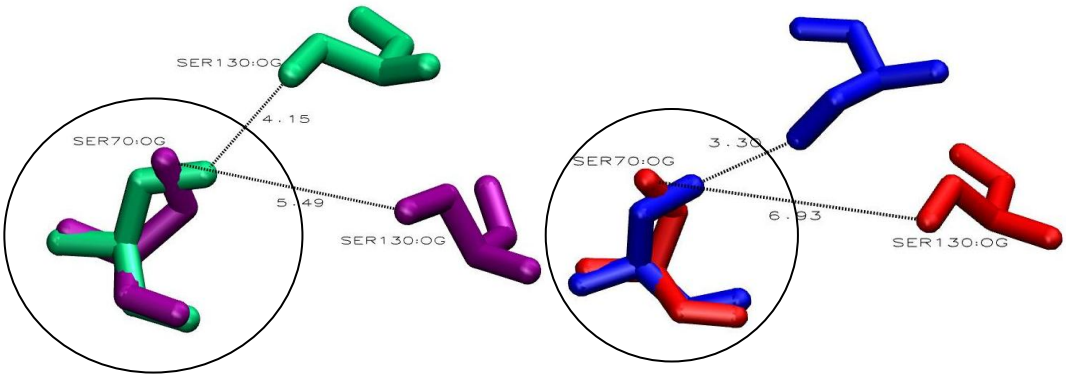

Figure. 3.19. Active site residues of TEM-1 β-lactamase. A. Ser 70 and Ser 130 in TEM-1-peptide simulations. B. Ser 70 and Ser 130 residues in TEM-1 - BLIP simulations.

Figure 3.19 shows the interaction between Serine 70 and Serine 130 for the simulations of TEM-1 in complex with wild type and mutant substrate. In Figure 3.19.A. Ser 70 and Ser 130 residues of TEM-1 β-lactamase in TEM-1-peptide and TEM-1 mutant peptide (D49A) are shown in green and purple, respectively. In Figure 3.19.B. Ser 70 and Ser 130 residues of TEM-1 β-lactamase in TEM-1 - BLIP and TEM-1 - mutant BLIP (D49A) are shown in blue and red, respectively.

When residue Asp49 of BLIP is mutated to Ala, the interaction between the active site residues Ser70 and Ser 130 is also affected. The distance between the atoms increases as a result of the mutation for both BLIP and the BLIP based peptide.

3.4.3. Ser 70 – Lys234

According to the distance values between the TEM-1 BLIP , TEM-1 peptide complexes and their mutant ones , it was determined that another attention should be paid on Ser 70 and Lys 234. The interaction between these residues show significant differences in terms of distance between their atoms.

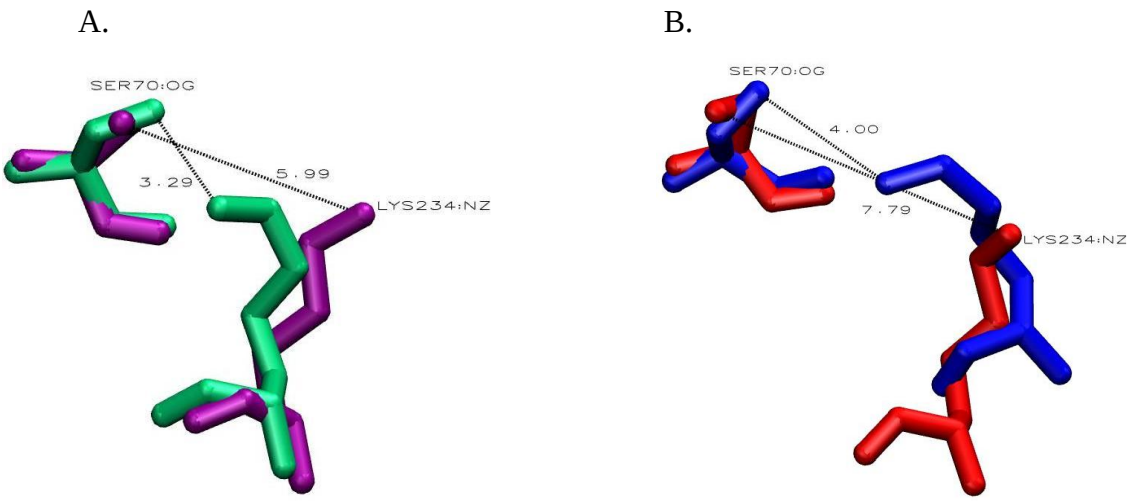

Figure 3.20. Active site residues of TEM-1 β-lactamase. A. Ser 70 and Lys 234 in TEM-1-peptide simulations. B. Ser 70 and Lys 234 residues in TEM-1 - BLIP simulations.

Figure 3.20 shows the interaction between Serine 70 and Lysine 234 for the simulations of TEM-1 in complex with wild type and mutant substrate. In Figure 3.20.A. Ser 70 and Lys 234 residues of TEM-1 β-lactamase in TEM-1-peptide and TEM-1 mutant peptide (D49A) are shown in green and purple, respectively. In Figure 3.20.B. Ser 70 and Lys 234 residues of TEM-1 β-lactamase in TEM-1 - BLIP and TEM-1 - mutant BLIP (D49A) are shown in blue and red, respectively.

3.5. Binding Free Energy Calculations

The binding free energies for the TEM-1 – BLIP and TEM-1 – mutant BLIP complexes were estimated by MM-PBSA method using APBS software. The calculated binding free energies are listed in Table 3.4

Table 3.4. Binding Free Energy components of TEM-1 BLIP complex and TEM-1 mutant BLIP complex simulations obtained by APBS.

Energy	TEM - BLIP	TEM- mutant BLIP
<ΔGnp>	276.23	267.95
<ΔGPB>	$-18.47*10^3$	$-18.15*10^3$
<ΔEvdW>	$43.08*10^3$	$43.44*10^3$
<ΔEelec>	$-18.37*10^5$	$-18.71*10^5$
<ΔEint>	$10.30*10^3$	$10.39*10^3$

Nonpolar solvation energy (ΔG_{np}) and van der Waals energies (ΔG_{vdW}) were found to be unfavorable for TEM-1 BLIP binding. According to Table 3.1 it can be said that the favorable formation of these complexes are driven by the polar contributions to solvation with a negative value of $-18,47*10^3$ kj/mol and $-18,15*10^3$ kj/mol and electrostatic interactions again with a negative value of $-18,37*10^5$ kj/mol and $-18,71*10^5$ kj/mol for the TEM-1 BLIP and TEM-1 mutant BLIP complexes. ΔG value is estimated as $-1.789*10^5$ kj/mol for TEM-1-- BLIP complex and $-1.427*10^5$ kj/mol for TEM-1 - BLIP (D49A) complex, suggesting that the binding of TEM-1 BLIP complex is a tighter binding compared to the binding of TEM-1 to mutant BLIP complex. The results confirm the importance of Asp 49 residue in terms of binding.

4. EXPERIMENTAL METHODS

4.1. Cloning of BLIP gene

4.1.1. Extraction of genomic DNA

Genomic DNA from *S. clavuligerus* was isolated using FERMENTAS genomic DNA isolation kit.

200 µl of sample was mixed well with 400µl of lysis solution and incubated at 65°C for 5 min. 600µl of chloroform was immediately added, gently emulsified by inversion (3-5 times) and centrifuged at 10,000 rpm for 2min. Precipitation solution was prepared by mixing 720µl of sterile de ionized water with 80µl of supplied 10x concentrated solution. Then, the upper aqueous phase containing DNA was transferred to a new tube. 800µl of fresh prepared precipitation solution was added. The sample was mixed gently by several inversions at room temperature for 1-2 min and centrifuged at 10,000rpm for 2min. Supernatant was removed completely and DNA pellet was dissolved in 100µl of 1.2M NaCl solution by gentle vortexing. After being sure that pellet was completely dissolved, 300µl of cold ethanol was added in order to let the DNA precipitate (10min at - 20°C) and the sample was spun down (10,000rpm, 3-4min) and ethanol was poured off. The pellet was washed once with 70% cold ethanol and DNA was dissolved in 100µl of sterile deionized water by gentle vortexing.

4.1.2. Amplification of BLIP gene

This genomic DNA was used as the template for the amplification of the 498 base pair BLIP gene using polymerase chain reaction (PCR). The forward and reverse primers with flanking *Nco*I and *Hind*III sites have been used. The primers are given in Table 4.1 with the highlighted enzyme sites.

Table 4.1. Primers used for the amplification of BLIP gene

Name	Purpose	Sequence
BIFpe	Forward primer	**CAT GCC ATG GAT GCG GGG GTG ATG ACC GG**
BLIPr	Reverse primer	**CAC AAG CTT TAC AAG GTC CCA CTG CCG**

Melting temperature was calculated as 69.4°C and 63.4°C for the forward and reverse primers, respectively, using Equaiton 4.1. Amplification reaction was performed after pre-heating at 95°C for 10 min then 30 cycles of heating at 95°C for 30 seconds, annealing at 60°C for 30 seconds and elongation at 72°C for 1.5 minutes. The PCR reactions were carried out in a reaction volume of 50 µl containing 12.5 pmole of both forward and reverse primers, 5 µl of 10X buffer with 25mM $MgCl_2$, 0.25mM dNTP, 1.25 unit of *Pfu* DNA polymerase and 0.2 µg of *S. clavuligerus* genomic DNA

$$T_m = 64.9 + (41 * (G + C - 16.4/N)) \quad (4.1)$$

4.1.3. Purification of PCR products (BLIP gene)

Using FERMENTAS purification kit, the following protocol was followed for the purification of the PCR products. The volume for each PCR tube was adjusted to a total volume of 100 µl. 500 µl binding buffer was added to each 100 µl PCR tube. The samples were mixed well. One high pure filter tube was inserted into one collection tube. The sample was transferred to the upper reservoir of the filter tube. The sample was centrifuged 60 seconds at a maximum speed at room temperature. The filter tube was disconnected and the flowthrough solution was discarded. The filter tube was reconnected to the same collection tube and the column was washed with the provided buffer. The flowthrough solution and collection tube were discarded. the filter tube was connected to a clean 1.5 ml microcentrifuge tube and the DNA sample was eluted using 40 µl elution buffer.

4.1.4. Restriction Enzyme Digestion

The purified BLIP gene and the pET20b(+) plasmid were digested by and *Nco*I and *Hind*III restriction enzymes under the following conditions.

4.1.4.1. pET 20 b(+) Plasmid Digestion with restriction enzymes. Restriction by HindIII enzyme was performed in a total of 20 µl at 37°C for 1hour. The reaction mixture contained 20 units of HindIII enzyme, 2 µl of 10X Buffer and 0.5 µg of pET20-b(+) plasmid vector.

After purification of plasmid from this reaction mixture, the HindIII digested plasmid was digested with *Nco*I enzyme. This reaction was performed in a total volume of 60 µl at 37°C overnight. This reaction mixture contained 10 units of *Nco*I enzyme, 6 µl of 10X Buffer and 0.5µg of pET20-b(+) plasmid vector.

4.1.4.2. BLIP Digestion with restriction enzymes. Restriction of the BLIP gene by *Nco*I enzyme was performed in a total volume of 60 µl at 37°C overnight. The reaction mixture contained 10 units of *Nco*I enzyme, 6µl of 10X Buffer and 0.2.µg of BLIP gene. After purification of plasmid from this reaction mixture, digestion with second enzyme was carried out. Restriction by *Hind*III enzyme was performed in a total of 50 µl at 37°C for 1 hour incubation. The reaction mixture contained 20units of *Hind*III enzyme, 5µl of 10X Buffer and 0.2 µg (10ul) of BLIP gene.

4.1.5. DNA purification from restriction reactions

The following protocol was used for the cleaning of the plasmid and BLIP gene from the digestion reactions. 3 volumes of binding solution was added to 1 volume of sample. Then the resuspended silica powder suspension was added. Up to 2.5µg of DNA, 5µl of silica powder suspension was added. The mixture was incubated for 5 minutes at 55°C and vortexed every 2min to keep silica powder in suspension. The silica powder/DNA complex was spinned for 5 seconds to form a pellet and the supernatant was removed. The pellet

was washed with 500µl of ice cold wash buffer three times. During each washing the pellet was resuspended completely. After the supernatant from the last wash has been removed, the tube was spinned again and the remaining liquid was removed with a pipette and the pellet was air-dried for 10-15min. The DNA was eluted with TE buffer by resuspending the pellet in an aliquot of TE and the tube was incubated at 55°C for 5 minutes. The tube was spinned and the supernatant was removed into a new tube avoiding the pellet.

4.1.6. Ligation of the BLIP gene and the pET20b(+) plasmid

The amplified BLIP gene was ligated into the linearized pET20b(+) plasmid using the following reaction condition. In a total volume of 20 µl in a microfuge tube the ligation mixture contained 150 ng BLIP gene, 40 µg pET20-b(+), 2 µl of 10X ligation buffer, and 3 units of ligase enzyme. The reaction mixture was incubated at 4°C overnight.

4.2. Transformation of pET20b(+) into *E.coli* by $CaCl_2$

The following protocol was used to transform *E. coli* XL1 or BL21(DE3) cells with the recombinant plasmids. A preculture of *E. coli* XLI cells was grown overnight in LB broth. This was used for inoculation into fresh LB broth at a 1:100 dilution (OD_{600} was kept below 0.05). Cells were grown at 37˚C with vigorous shaking in flasks to facilitate aeration. When the cells reached the optical density of 0.5 at 600 nm they were centrifuged at 3,000 rpm for 10 minutes in sterile tubes. The supernatant was discarded and the cells were resuspended in 100µl of sterile, ice-cold 0.1 M $CaCl_2$. The cells were incubated on ice for 30 minutes. The tube was mixed gently every 10 minutes to allow a homogenous mixture.10µl Ligation mixture or plamid preparation was added to the cells. The cells were then incubated on ice for 1 hour to allow the plasmid DNA to enter the cells. Following a heat shock at 42˚C for 60 seconds, the cells were further incubated on ice for 10 more minutes. 800 µl of LB broth without any antibiotics was added to 100 µl reactions. The cells were incubated at 37˚C for 1 hour. The transformed cells were centrifuged at 3000 rpm for 1-5 minutes and then plated on selective plates. The plates were incubated overnight at 37˚C.

4.3. Plasmid isolation

4.3.1. Mini-Prep Plasmid Isolation

ROCHE high pure plasmid isolation kit was used to obtain up to 20µg of plasmid DNA using the following procedure. The protocol allowed the preparation of DNA from 0.5 - 4.0 ml of *E. coli* culture with a density of 1.5-5.0 A600 units per ml.

250 µl suspension buffer containing RNase was added to the centrifuge tubes containing the bacterial pellet. The bacterial pellet was resuspended and mixed well. 250 µl lysis buffer was added and mixed gently by inverting the tube 3 to 6 times. The sample was incubated for 5 min at room temperature. 350 µl chilled binding buffer was added to the sample, and the contents of the tube was mixed gently by inverting the tube 3 to 6 times and incubated on ice for 5 minutes. Then, the solution became cloudy and a flocculant precipitate formed. The mixture was centrifuged for 10 min at approximately 13,000 x g in a standard tabletop microcentrifuge. After centrifugation, one high pure filter tube was inserted into one collection tube. The entire supernatant obtained after centrifugation was transferred into the upper buffer reservoir of the filter tube. The entire high pure tube assembly was inserted into a standard tabletop microcentrifuge. This was centrifuged for 1 min at full speed. After centrifugation, the filter tube was removed from the collection tube, flowthrough liquid was discarded and the filter tube was re-inserted in the same collection tube. The column was two times with wash buffer II. After discarding the flowthrough liquid, the entire high pure tube assembly was centrifuged for an additional 1 min. The collection tube was discarded. To elute the DNA, the filter tube was inserted into a clean, sterile 1.5 ml microcentrifuge tube.100 µl distilled water was added to the upper reservoir of the filter tube for elution. The tube assembly was centrifuged for 1 min at full speed.

4.3.2. Midi-Prep Plasmid Isolation

ROCHE genopure plasmid midi kit was used to obtain up to 100µg of plasmid DNA using the following procedure. DNA was isolated from overnight cultures of E. coli picked from single colonies.

Bacterial cells from 10 ml culture grown in LB medium were precipitated by centrifugation for 5 – 10 min at 3,000 – 5,000 × g, +4°C. The supernatant was discarded. The pellet was carefully resuspended in 4 ml suspension buffer containing RNase and mixed. 4 ml lysis buffer was added to the suspension and mixed gently by inverting the tube 6 to 8 times. This was incubated 2 – 3 min at room temperature. 4 ml chilled neutralization buffer was added to the suspension. The suspension was immediately mixed gently by inverting the tube 6 to 8 times until a homogenous suspension was formed. Then the tube was incubated 5 min on ice. The lysate was cleared by filtration.

The cleared lysate was loaded onto the equilibrated column and the column was allowed to empty by gravity flow. The flowthrough was discarded and the column was washed. Finally DNA was eluted using distilled water.

4.4. Restriction enzyme digestion for screening recombinant colonies

After transformation, recombinant colonies were selected on LB agar plates containing ampicillin. Following mini-prep plasmid isolation, the recombinant plasmids were confirmed by double digestion using the protocols given in section 1.1.4. The digestion products were checked using agarose gel electrophoresis and the colonies with the correct plasmid were selected.

4.5. Agarose Gel Electrophoresis of DNA

In order to visualize and quantify DNA fragments agarose gel electrophoresis was used. 1% (m/v) agarose gels were prepeared by boiling the appropriate amount of powdered agarose in 0.5X TBE buffer. Then ethidium bromide was added to a final concentration of 0.5µg/ml. Warm agarose was poured into the plastic tray supplied with the electrophoresis apparatus with a comb to create slots for sample loading. After the gel completely polymerized, the comb was removed carefully. The gel was placed in the electrophoresis tank filled with 0.5X TBE. The DNA samples were mixed with a loading dye and loaded into the slots of submerged gel. After running gel for 20 -30 minutes at 120V, the gel was examined under ultraviolet light and snapshots were taken.

4.6. Growth of Recombinant *E. coli* Cells and Expression of Recombinant Proteins

Recombinant *E. coli* cells were grown in LB medium medium containing 100 mμ/ml ampicillin for the selection of the plasmid harbouring cells at 180 rpm in 37°C. Growth was monitored by measuring the optical density at 600 nm using a spectrophotometer. When the OD_{600} reached to a set value (0.2), the cells were induced with isopropyl β-D-1-thiogalactopyranoside (IPTG) and growth was further monitored.

5. MATERIALS

5.1. Bacterial Strains and Plasmids

S. clavuligerus was purchased from DSMZ. *E. coli* XL-1 and *E. coli* BL21(DE3) cells was from our laboratory stock. All *E. coli* strains were grown in LB medium that contained ampicillin when required for the maintenance of plasmid DNA.

5.2. Chemicals and Enzymes

All chemicals and solutions used in this study were purchased from MECK (Germany) or SIGMA (USA). The restriction endonucleases were from New England Biolabs (USA) or Fermentas.

5.3. Laboratory Equipments

Table 5.1. List of Laboratory Equipments

Absorbance measurement	DU 640 spectrophotometer (Bechman, USA)
Agarose gel electrophoresis	Mini-Sub Cell GT (Biorad, USA)
Centrifugation	1-15 centrifuge (SIGMA, Germany) J26-XPIAVATIcentrifuge(Beckman Coulter,USA)
Deepfreezers	New Brunswick Scientific Ultra Low Temperature Freezer U410 Pemium (USA)
Ice Machine	FBOC Icematic
Incubation	FN500 Incubator (Nüve, Turkey) Environmental Shaker Incubator ES-20, (Biosan, Latvia)
Sterilization	Autoclave (ALP, Japan)
pH measurement	pH meter, SCHOTT, Germany
Pipetting	1-10, 10-100, 100-1000 µl pipets (Thermo electron corporation, CANADA)
Power Supply	Power EC250 – 50 (Thermo electron corporation, CANADA)
Refrigerating	Refrigerator, Frigidaire (Ohio, USA)
Sterile Environment	Laminair (Holten, Denmark)
UV light	UV Lamb, Biolab (USA)
Vortexing	Reax Vortex (Heidolph, Germany)
Weighing	Balance XB 220A (Precisa, Switzerland)

5.4. Growth Media for *Escherichia coli*

Table 5.2. LB Medium

Chemical	**Amount**
Tyrptone	10g
Yeast Extract	5g
NaCl	10g

Table 5.3. LB Agar Medium

Chemical	**Amount**
Tyrptone	10g
Yeast Extract	5g
NaCl	10g
Agar	15g

5.5. Buffers and Solutions

Table 5.4. 10X TBE Buffer

Chemical	**Amount**
Trisma Base	445mM
EDTA	10mM
Boric Acid	445mM

5.6. Kits

DNA extraction kit was purchased from Fermentas and High Pure PCR Product Purification Kit, Genopure Plasmid Midi Kit and High Pure Plasmid Isolation Kit was purchased from Roche.

6. RESULTS AND DISCUSSION

6.1. Cloning of BLIP gene

The pET System is a very powerful system developed for the cloning and expression of recombinant proteins in *E. coli*. Target genes are cloned in pET plasmids under control of strong bacteriophage T7 transcription and (optionally) translation signals; expression is induced by providing a source of T7 RNA polymerase in the host cell. T7 RNA polymerase is so selective and active that, when fully induced, almost all of the cell's resources are converted to target gene expression; the desired product can comprise more than 50% of the total cell protein a few hours after induction. Once established in a non-expression host, target protein expression may be initiated by transferring the plasmid into an expression host containing a chromosomal copy of the T7 RNA polymerase gene under *lacUV5* control. In this case, expression is induced by the addition of IPTG to the bacterial culture. Although in some cases (e.g., with innocuous target proteins) it may be possible to clone directly into expression hosts, this approach is not recommended (Stratagene).

The pET-20b(+) vector was chosen for cloning the BLIP gene in this work. It has an N-terminal *pel*B signal sequence for potential periplasmic localization and an optional C-terminal His•Tag sequence (Figure 6.1) for affinity purification using nickel column. The unique sites containing the polycloning region is indicated on Figure 6.1.

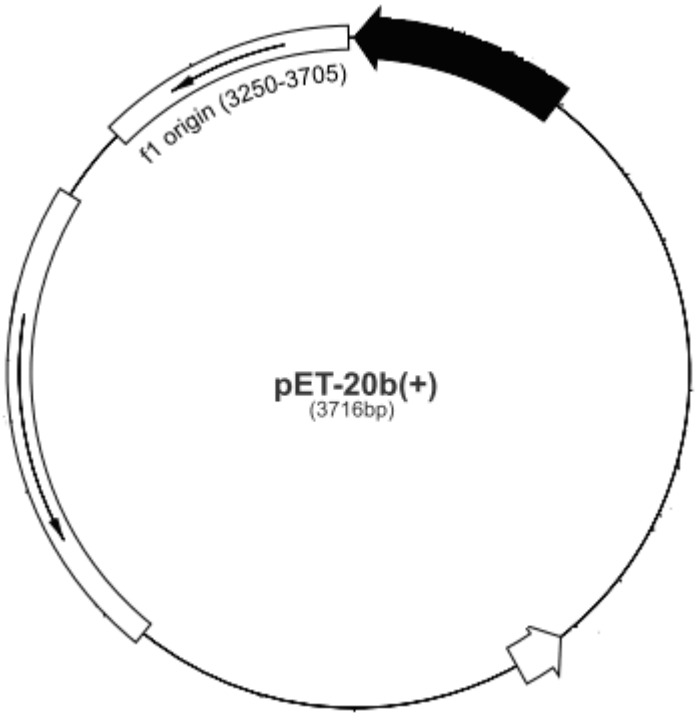

Figure 6.1. pET20-b(+) plasmid vector

β-lactamase is a periplasmic protein. Therefore in order for BLIP to bind β-lactamase BLIP should also be transported to the periplasmic space. In its original host BLIP is also a periplasmic protein. However since it was not clear if the same signal sequence could be recognized by *E. coli* secretion machinery, it was more convenient to use a signal sequence such as *pel*B which was recognized by the *E. coli* secretion machinery. For this reason pET20b(+) vector was chosen in this study.

A powerful feature of the pET system is the ability to clone target genes under conditions of extremely low transcriptional activity, that is, in the absence of a source of T7 RNA polymerase. Background expression is minimal in the absence of T7 RNA polymerase because the host RNA polymerases do not initiate from T7 promoters and the cloning sites in pET plasmids are in regions weakly transcribed (if at all) by read-through activity of bacterial RNA polymerase. Even low levels of basal expression can cause difficulties in growth and plasmid instability in these expression hosts due to transcription from the T7 promoter in the pET plasmids (Stratagene). Therefore in this work *E. coli* XL1 strain was used as the cloning host.

For protein production, the recombinant plasmid was transferred to the *E. coli* BL21(DE3) strain containing a chromosomal copy of the gene for T7 RNA polymerase. It has the promoter to direct transcription of the T7 RNA polymerase gene. This promoter is inducible by isopropyl-β-D-thiogalactopyranoside (IPTG).

6.1.1. Pimer Design

BLIP gene was amplified using the *S. clavuligerus* genomic as the template by PCR as described in section 1.2. The primers were designed using the sequence information published by Stratagene reference. In designing the forward primer, the 108 base pair BLIP gene signal sequence was omitted and the BLIP gene was inserted downstream from the *pelB* sequence.

*Nco*I was selected as a restriction enzyme for the the design of 5’ amino terminal primer. It was 29 nucleotides long, and its sequence was determined as: 5’ CAT GCC ATG GAT GCG GGG GTG ATG ACC GG ’3. The first 6 nucleotides were extrinsic to the gene and the created the underlined *Nco*I restriction endonuclease gene site. *Hind*III was selected as a restriction enzyme for the design of the 3’ carboxyl terminal primer and its sequence was determined as: 5’ CAC AAG CTT TAC AAG GTC CCA CTG CCG 3’. The first 1 nucleotide were extrinsic to the gene and the created the underlined *Hind*III restriction endonuclease gene site. NEB Cutter was used to obtain the restriction sites on this protein. (web sitesi). The specifications of the designed primers are shown in the Table 6.1.

Table 6.1. Specification of designed primers

Specification	Forward Primer	Reverse Primer
GC Content	65.5 %	55.5 %
DNA Bases	29	27
Molcular Weight	9039.9	8189.4
Tm	69.4˚C	63.4˚C

6.1.2. Optimization of PCR conditions

The fragment containing the BLIP gene was amplified using the primers described in section 4.1.2. Various concentrations of *S.clavuligerus* genomic DNA, and Mg^{+2} concentrations were used with *Pfu* DNA polymerase. The presence of a single bright band was observed with following conditions. 5 µl of 10X buffer with 25mM $MgCl_2$, 0.25mM dNTP, 1.25unit of *Pfu* DNA polymerase and 0.2 µg of *S. clavigerous* genomic DNA. The amplified 498 base pair BLIP gene is given in Figure 6.2.

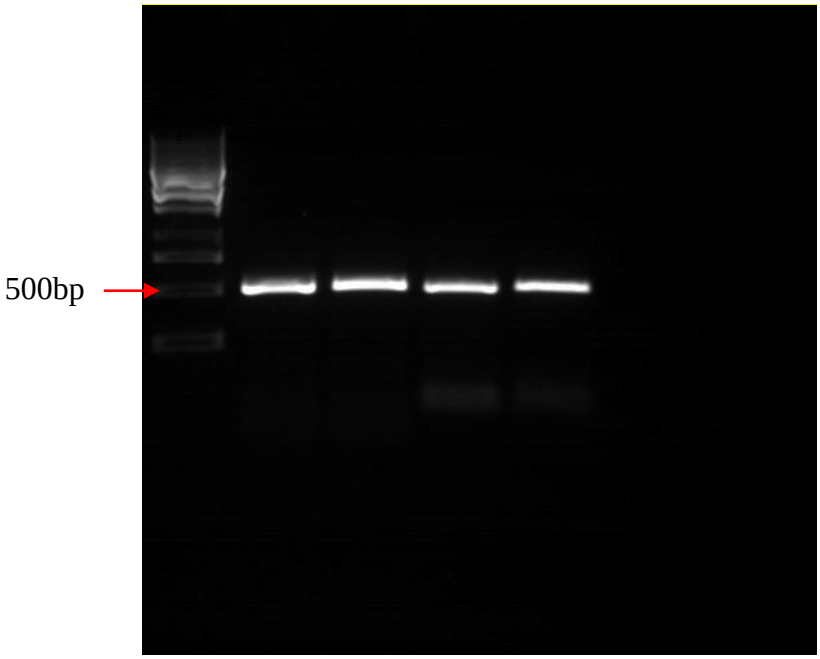

Figure. 6.2. Electrophoretic analysis of amplified BLIP which is 498bp on agarose gels.

6.1.4. Construction of the Recombinant Plasmid

The BLIP gene was amplified using the optimized PCR conditions and then purified from the reaction mixture. Then it was digested with *Hind*III and *Nco*I restriction enzymes, respectively. The digestion product was than ligated with the pET-20b(+) plasmid vector which has also been linearized with the same restriction enzymes. The agarose jel electrophoresis of the linearized plasmid and the BLIP gene before ligation are given in Figure 6.3.

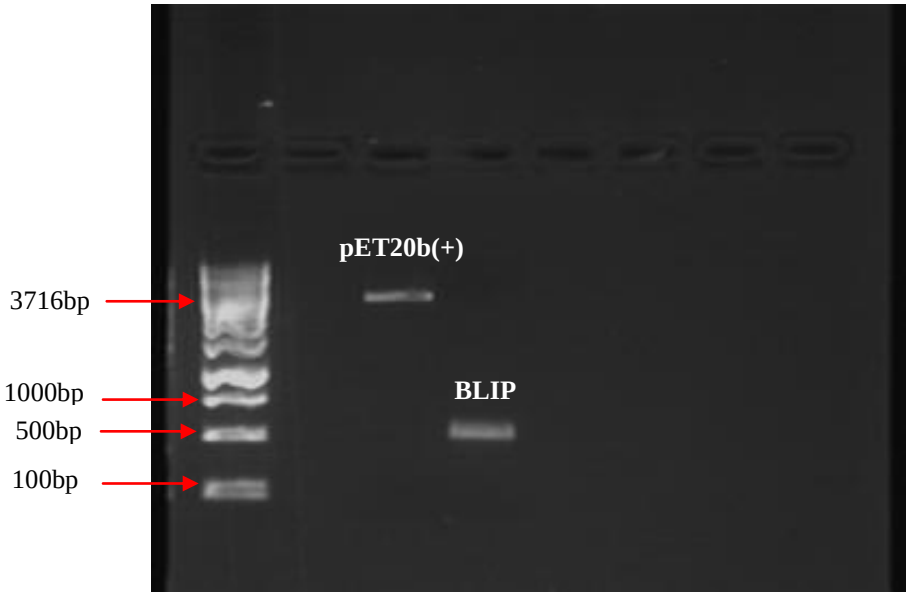

Figure 6.3. Electrophoretic analysis of the double digested BLIP gene and the linearized pET20b(+) before the ligation on agarose gel.

6.2. Screening of the Recombinant Colony

After ligation, transformation was carried out with *E. coli* XL1 cells. In order to confirm the presence of the BLIP gene in the plasmid vector, transformants were selected on LB agar plates containing medium containing 100mμ/ml ampicillin. The next step was to perform mini plasmid isolation and restriction enzyme analysis. Restriction analysis was used to confirm that the new construct harbored the BLIP gene. The results of the analysis are presented on Figure 6.4.

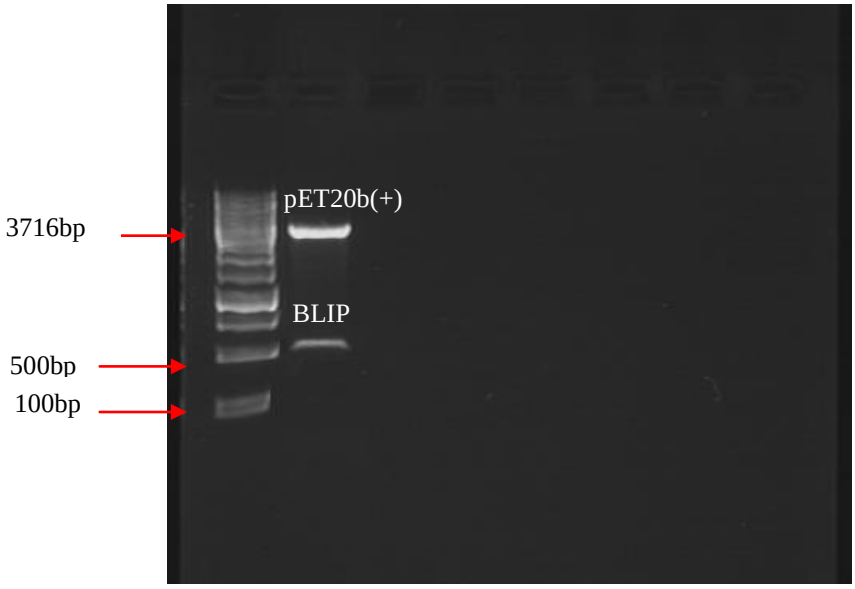

Figure 6.4. Electrophoretic analysis of isolated recombinant colony on agarose gel

As also clear from this figure, after a double digest of the possible recombinant plasmid with *Hind*III and *Nco*I enzymes, a band corresponding to the BLIP gene was apparent on the jel. This new recombinant plasmid was named as pPKblip.

6.3. Expression of the BLIP gene

The recombinant plasmid was selected from *E.coli* XL1 cells. However for expression of the BLIP protein *E. coli* BL21(DE3) strain was first transformed with this plasmid. These cells were grown on LB agar plates with 100mμ/ml ampicilin for the selection of the cells harboring the recombinant plasmid. *E. coli* BL21(DE3) cells containing the recombinant plasmids was then grown in LB medium containing 100μg/ml ampicillin. When OD_{600} reached a value of 0.2, 1mM IPTG was added to the medium. Whereas β-lactamase expression was constitutive, BLIP expression was under the control of IPTG induction. Duplicate experiments to analyze the possible *in-vivo* interaction were conducted.

Upon induction with IPTG it was expected for BLIP to be expressed and translocated to the periplasm. BLIP in this compartment should supposedly find β-lactamase and bind it inhibiting its action. This should cause the growth to cease since ampicillin, the β-lactam

antibiotic in the growth medium, will not be rendered inactive and attack the cell wall. Although, the cell growth was expected to decelerate after induction with IPTG, induced *E.coli* cells showed only small decreases in their growth. Figure 6.4 shows the growth curve of *E.coli* cells. As it was expected, it can bee seen from the figure that uninduced cells grew exponentially during 12 hour experiment. However, induced cells show little decrease in their growths which is not expected if *in vivo* binding of BLIP would really occur.

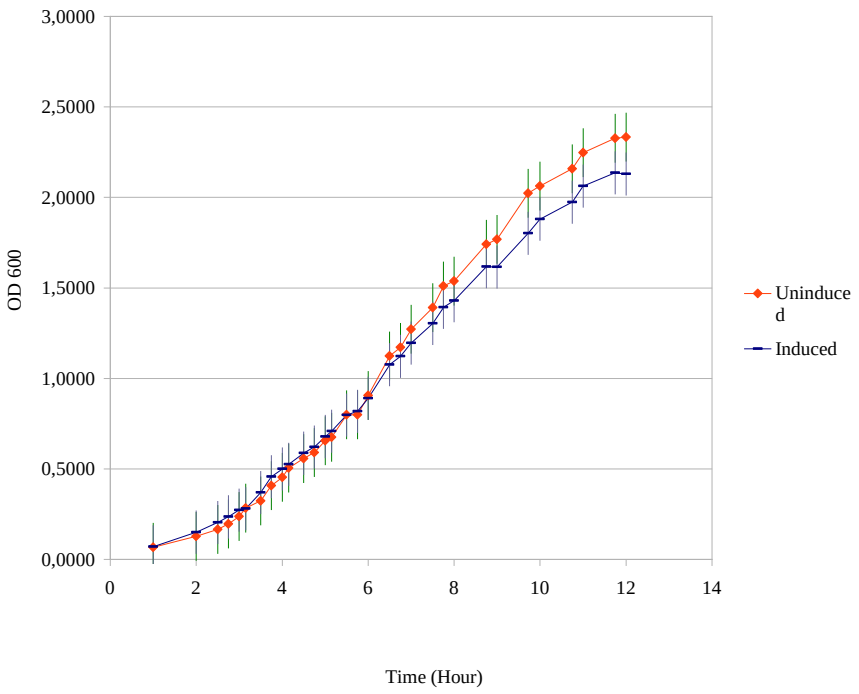

Figure 6.4. Growth curve of the recombinant XL1 (pET20b(+) cells with IPTG induction(yellow) and without IPTG induction (red).

7. CONCLUSIONS AND RECOMMENDATION FOR FUTURE STUDIES

7.1. Conclusions

Molecular dynamics simulations of free TEM-1 as well as TEM-1 in the presence of 1. BLIP, 2. mutant BLIP (D49A), 3. Peptide 1: BLIP based peptide (HAAG**D**YYA), 4. Peptide 2: BLIP based mutant peptide (HAAG**A**YYA) and 5. Peptide 3: peptide based on the loop 2 region of BLIP (FYRGSAHLWFY) were carried out. The RMSD profiles of these simulations show that all simulations reach equilibrium. In TEM-1 - peptide complex simulations, the peptide based on the 142-152 region of BLIP showed significant deviations from the initial structure, suggesting that the peptide based on residues 45-52 of BLIP may be a better choice for the ultimate purpose, which is the design of new peptide inhibitors.

When trajectories are analyzed and MSF values of the residues are examined, it is observed that in all cases, as is usual in the MD of proteins, the main contribution to the motion is localized in loops connecting the secondary structure elements (i.e residues 51 to 54, 84 to 89, 99 to 112, 161 to 179,193 to 203).

Asp49 residue on BLIP and the BLIP based peptide was mutated to alanine to determine the contribution of this residue to binding. Simulations on the complex structures showed that similar conformational changes occur in the active site of TEM-1 β-lactamase as a result of D49A mutations in BLIP and the peptide. The D49A mutation also alters the mobility of the structures. In the residue based MSF plots it can be observed that as a result of D49A mutation, the largest fluctuations were observed in residue 176 of the omega loop, which forms one edge of the catalytic site. In addition, in the TEM-1 – peptide 2 (mutant peptide 1) complex simulation the flexibility of TEM-1 Val216 shows significant increase compared to TEM-1 peptide 1 complex simulation. Val216 of TEM-1 has van der Waals interactions with BLIP Tyr 50, which is the neighbor of Asp49. The results suggest that Asp 49 mutation affects the interaction between the Tyr50 of BLIP and

Val216 of TEM-1. In addition, the mutation of Asp49 of BLIP to Ala causes the Alanine residue to go toward 99-112 loop of TEM-1 and this behaviour results in a loss of interaction between the 49th residue of BLIP and the active site region of TEM-1.

Binding free energy of the TEM-1 BLIP and TEM-1 mutant BLIP (D49A) complexes was estimated by the molecular mechanics Poisson Boltzmann Surface Area (MM-PBSA) method. The binding free energy of TEM-1 BLIP complex was lower than that of the TEM-1 mutant BLIP complex, indicating the contribution of the Asp49 residue of BLIP to tight binding

In the experimental section of the study the *in-vivo* binding of BLIP from *S. clavuligerus* to R-TEM-1 β-lactamase and its inhibition under these physiological conditions were examined by cloning. β-lactamase is a periplasmic protein therefore BLIP was also constructed with a signal sequence to enable its periplasmic transport. β-lactamase was produced constitutively but BLIP expression was induced by IPTG addition. As the cells entered logarithmic growth phase, BLIP expression was induced. Consequently, a retardation in growth was expected due to the inactivation of β-lactamase. The growth profile of *E. coli* BL21(DE3) cells indicated that growth was indeed retarded slightly after induction. This decrease in growth may be related to inhibition of TEM-1 β-lactamase by BLIP but it may also be due to the metabolic burden of heterogonous protein (BLIP) expression and not because of the BLIP binding to β- lactamase. The slight decrease in growth rate may be because BLIP was not translocated to the periplasm, therefore could not bind β-lactamase. Another reason could be that it was translocated to the periplasmic space but could not recognize β-lactamase. Finally it was also possible that the two proteins bound each other but β-lactamase was still effective in rendering the lethal effect of the β-lactam antibiotic, ampicillin.

7.2. Recommendations for Future Studies

Further computational studies can be performed with different peptides in order to find the best TEM-1 β-lactamase inhibitor. Different residue mutations can be performed to propose the tight binding peptides. The TEM-1 – peptide complex simulation times can be extended to achieve better convergence for free energy calculations.

There are four class of β-lactamases. In order to gain a better understanding about class specific characteristics of β-lactamase - peptide recognition, inhibitory properties of peptides against different β-lactamases can be determined. As a first step, SHV-1 β-lactamase, which is known to share 67 per cent sequence identity with TEM-1 β-lactamase, can be used to obtain a comparison between TEM-1 and SHV-1 ligand recognition.

As a first step of the investigation of *in vivo* inhibiton of β-lactamases by newly designed peptides, *in vitro* verification of these peptides can be carried out by kinetic studies

After designing the strongest binding peptide, peptide delivery inside the cell can be pursued.

APPENDIX A: INPUT FILES USED IN COMPUTATIONAL STUDIES

NAMD Configuration File

```
#############################################################
## JOB DESCRIPTION                                         ##
#############################################################

# Minimization and Equilibration of
# TEM1-BLIP in a Water Box

#############################################################
## ADJUSTABLE PARAMETERS                                   ##
#############################################################

structure          ../ionizedTEMBLIP.psf
coordinates        ../ionizedTEMBLIP.pdb


set temperature    300
set outputname     complex_wb_eq
set init_temp      50
firsttimestep      0

#############################################################
## SIMULATION PARAMETERS                                   ##
#############################################################



# Input
paraTypeCharmm          on
parameters          ../toppar/par_all27_prot_lipid.prm
temperature         $init_temp


# Force-Field Parameters

exclude             scaled1-4
1-4scaling          1.0
cutoff              12.
switching           on
switchdist          10.
pairlistdist        13.5

# Integrator Parameters
```

```
timestep            1.0  ;# 1fs/step
rigidBonds          all  ;# needed for 2fs steps
nonbondedFreq       1
fullElectFrequency  2
stepspercycle       10



# Constant Temperature Control

langevin            on    ;# do langevin dynamics
langevinDamping     5     ;# damping coefficient (gamma) of 5/ps
langevinTemp        $init_temp
langevinHydrogen    off    ;# don't couple langevin bath to hydrogens



# Periodic Boundary Conditions

cellBasisVector1     81.55100059   0.   0.
cellBasisVector2     0.   79.43899917  0.
cellBasisVector3     0.    0.  87.30799913
cellOrigin           15.4557247162 27.078086853 51.3710594177
margin               2.5
wrapAll              on



# PME (for full-system periodic electrostatics)

PME                  yes
PMEGridSizeX         90
PMEGridSizeY         80
PMEGridSizeZ         90



# Constant Pressure Control (variable volume)

useGroupPressure     yes ;# needed for rigidBonds
useFlexibleCell      no
useConstantArea      no

langevinPiston       on
langevinPistonTarget  1.01325 ;#  in bar -> 1 atm
```

```
langevinPistonPeriod  100.
langevinPistonDecay   50.
langevinPistonTemp    $init_temp


# Output

outputName          $outputname
restartfreq         500     ;# 500steps = every 1ps
dcdfreq             250
xstFreq             250
outputEnergies      100
outputPressure      100


##############################################################
## EXTRA PARAMETERS                                         ##
##############################################################

constraints on
consexp 2
consref   ../ionizedTEMBLIP.pdb
conskfile ../ionizedTEMBLIP_cons.pdb
conskcol B
constraintScaling 5

##############################################################
## EXECUTION SCRIPT                                         ##
##############################################################

# turn off until later
#langevinPiston                    off


# Minimization

minimize            1000
output mini.cons5


cnstraintScaling 3
minimize            1000
output mini.cons3



constraintScaling 0
minimize            1000
```

```
output mini.all


reinitvels      $init_temp

run             4000
for { set TEMP [expr ($init_temp + 10)] } { $TEMP < $temperature } { incr TEMP 10
} {
   langevinTemp          $TEMP
   LangevinPistonTemp   $TEMP
   run                   4000
}

langevinTemp          $temperature
#LangevinPistonTemp   $TEMP
run                   5000000
```

PGN File used to build the PSF file

```
package require psfgen
topology top_all27_prot_lipid.inp
pdbalias residue HIS HSE
pdbalias atom ILE CD1 CD
segment TEM {pdb tem.pdb}
coordpdb tem.pdb TEM
segment pep {pdb blip.pdb}
coordpdb blip.pdb pep
guesscoord
writepdb temblip.pdb
writepsf temblip.psf
```

Tk Scripting

Distance.tcl

```
proc distance {molid residue1 type1 residue2 type2} {
set a1 [atomselect $molid "chain B and resid $residue1 and name $type1"]
set a2 [atomselect $molid "chain A and resid $residue2 and name $type2"]
set ind1 [$a1 get index]
set ind2 [$a2 get index]
label add Bonds $molid/$ind1 $molid/$ind2 }
```

namdstats.tcl

```
puts "Usage: data_avg <logfile> \[<first timestep> <last timestep>]"
puts "   <first timestep> and <last timestep> may be entered as numbers or"
puts "   <first timestep> = 'first' will start at the beginning of the simulation"
puts "   <last timestep> = 'last' will go to the end of the simulation"
puts "Usage: data_time <data stream> <logfile> \[<first timestep> <last timestep>]"
puts "   <data stream> = BOND, ANGLE, DIHED, IMPRP, ELECT, VDW, BOUNDARY,
MISC, KINETIC, TOTAL, TEMP, TOTAL2, TOTAL3, TEMPAVG"


proc data_avg {logfile {first 0} {last -1}} {

set file [open $logfile r]
while { [gets $file line] != -1 } {
  if [regexp "ETITLE:" $line] {set etitles $line}
  }
close $file
puts "Calculating averages..."

set file [open $logfile r]
set ener " "
while { [gets $file line] != -1 } {
  if [regexp "ENERGY:  " $line] {set ener "$ener $line"}
  }
close $file

set l [llength $etitles]
set lc [expr [llength $ener]/$l]

for {set k 0} {$k < $l} {incr k} {
  set tstest [lindex $etitles $k]
  if {$tstest == "TS"} {set tsnum $k}
  }

for {set k 0} {$k < $lc} {incr k} {
  set ts([expr $k+1]) [lindex $ener [expr $l*$k+$tsnum]]
```

```
  }
set lastts $ts($k)
set lastline $lc
set firstts $ts(1)
set firstline 1

if {$first != "first"} {
  set k 1
  while {$first > $ts($k)} {
    set firstts $ts([expr $k+1])
    set firstline [expr $k+1]
    incr k
    }
  }

if {$last != "last"} {
  set k 1
  while {$last >= $ts($k)} {
    set lastts $ts($k)
    set lastline $k
    incr k
    }
  }

puts "CALCULATING DATA FROM TIMESTEP $firstts TO $lastts:"

set k 0
for {set i 1} {$i <= $lc} {incr i} {
  for {set j 1} {$j <= [llength $etitles]} {incr j} {
    set e($i,$j) [lindex $ener $k]
    incr k
    }
  }

for {set j 3} {$j <= [llength $etitles]} {incr j} {
  set total 0
  for {set i $firstline} {$i <= $lastline} {incr i} {
    set total [expr $total + $e($i,$j)]
    }
  set avg [expr $total/(1+$lastline-$firstline)]
  puts "[lindex $etitles [expr $j-1]]: $avg"
  }

unset ener
unset ts
}


proc data_time {data logfile {first 0} {last -1}} {
```

```
set file [open $logfile r]
while { [gets $file line] != -1 } {
  if [regexp "ETITLE:" $line] {set etitles $line}
  }
close $file
puts "Getting $data data..."

set file [open $logfile r]
set ener " "
while { [gets $file line] != -1 } {
  if [regexp "ENERGY:  " $line] {set ener "$ener $line"}
  }
close $file

set lc [expr [llength $ener]/[llength $etitles]]

set k 0
for {set i 1} {$i <= $lc} {incr i} {
  for {set j 1} {$j <= [llength $etitles]} {incr j} {
    set e($i,$j) [lindex $ener $k]
    incr k
    }
  }

set lastts $e($lc,2)
set lastline $lc
set firstts $e(1,2)
set firstline 1

if {$first != "first"} {
  set k 1
  while {$first > $e($k,2)} {
    set firstts $e([expr $k+1],2)
    set firstline [expr $k+1]
    incr k
    }
  }

if {$last != "last"} {
  set k 1
  while {$last >= $e($k,2)} {
    set lastts $e($k,2)
    set lastline $k
    incr k
    }
  }

set j 0
```

```
switch $data {
  BOND {set j 3}
  ANGLE {set j 4}
  DIHED {set j 5}
  IMPRP {set j 6}
  ELECT {set j 7}
  VDW {set j 8}
  BOUNDARY {set j 9}
  MISC {set j 10}
  KINETIC {set j 11}
  TOTAL {set j 12}
  TEMP {set j 13}
  TOTAL2 {set j 14}
  TOTAL3 {set j 15}
  TEMPAVG {set j 16}
  default {
    puts "Invalid data stream selection"
    }
  }
if {$j != 0} {
  set file [open $data.dat w]
  for {set i $firstline} {$i <= $lastline} {incr i} {
    puts $file "$e($i,2) $e($i,$j)"
    }
  close $file
  }
unset ener
puts "Done"
}
```

APBS

APOLAR INPUT FILE

```
read

 mol pqr 0.pqr
mol pqr 0_tem.pqr
mol pqr 0_blip.pqr

    parm flat vparam-amber-parm94.dat
end


apolar name complex
grid 0.3 0.3 0.3
mol 1
srfm sacc
swin 0.3
srad 1.40
press 0
gamma 0.105
bconc 0.033428
sdens 100.0
dpos 0.2
temp 298.15
calcenergy total
calcforce no
end



apolar name tem

grid 0.3 0.3 0.3
mol 2
srfm sacc
swin 0.3
srad 1.40
press 0
gamma 0.105
bconc 0.033428
sdens 100.0
dpos 0.2
temp 298.15
calcenergy total
calcforce no
```

```
end
apolar name blip
grid 0.3 0.3 0.3
mol 3
srfm sacc
swin 0.3
srad 1.40
press 0
gamma 0.105
bconc 0.033428
sdens 100.0
dpos 0.2
temp 298.15
calcenergy total
calcforce no
end

print apolEnergy complex - tem - blip end


quit
```

POLAR INPUT FILE

```
read

   mol pqr 0_blip.pqr

end

elec name blip1

   mg-auto
   dime 161 97 129
   cglen 104.6384 73.7715 89.9283
   fglen 81.5520 63.3950 72.8990
   cgcent mol 1
   fgcent mol 1
   mol 1
   lpbe
   bcfl sdh
   pdie 2.0000
   sdie 78.5400
   srfm smol
   chgm spl2
   sdens 10.00
   srad 1.40
   swin 0.30
   temp 298.15
   calcenergy total
   calcforce no
end

elec name blip2

   mg-auto
   dime 161 97 129
   cglen 104.6384 73.7715 89.9283
   fglen 81.5520 63.3950 72.8990
   cgcent mol 1
   fgcent mol 1
   mol 1
   lpbe
   bcfl sdh
   pdie 2.0000
   sdie 2.0000
   srfm smol
   chgm spl2
   sdens 10.00
   srad 1.40
```

```
    swin 0.30

    temp 298.15
    calcenergy total
    calcforce no

end

print elecEnergy blip1 - blip2 end

quit
```

APPENDIX B: RESIDUE– RESIDUE DISTANCES IN THE MD SIMULATIONS

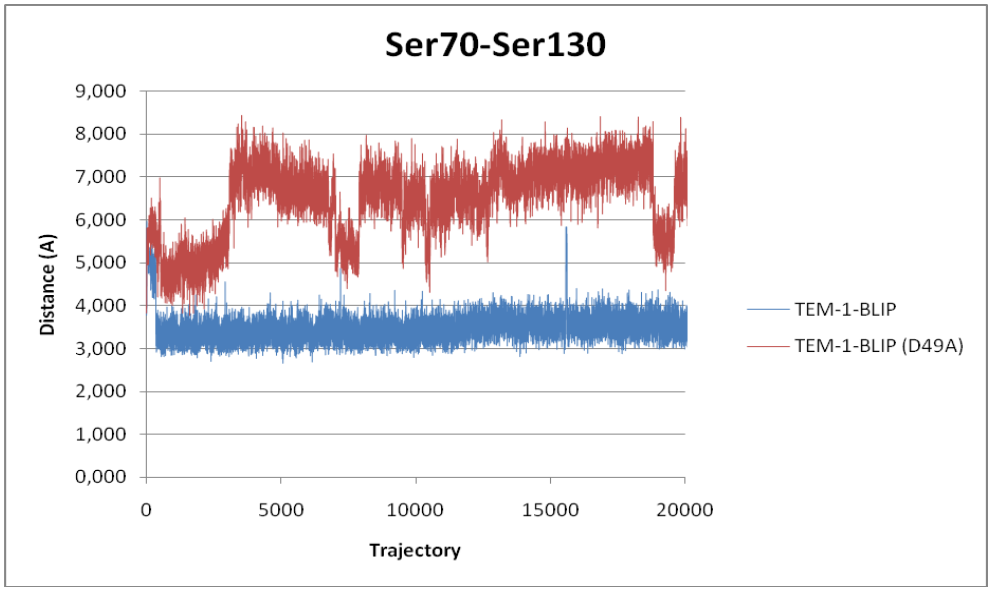

Figure B.1. Ser70 - Ser130 active site residue distances of TEM-1 – BLIP (blue) and TEM-1 – BLIP (D49A) (red) complexes.

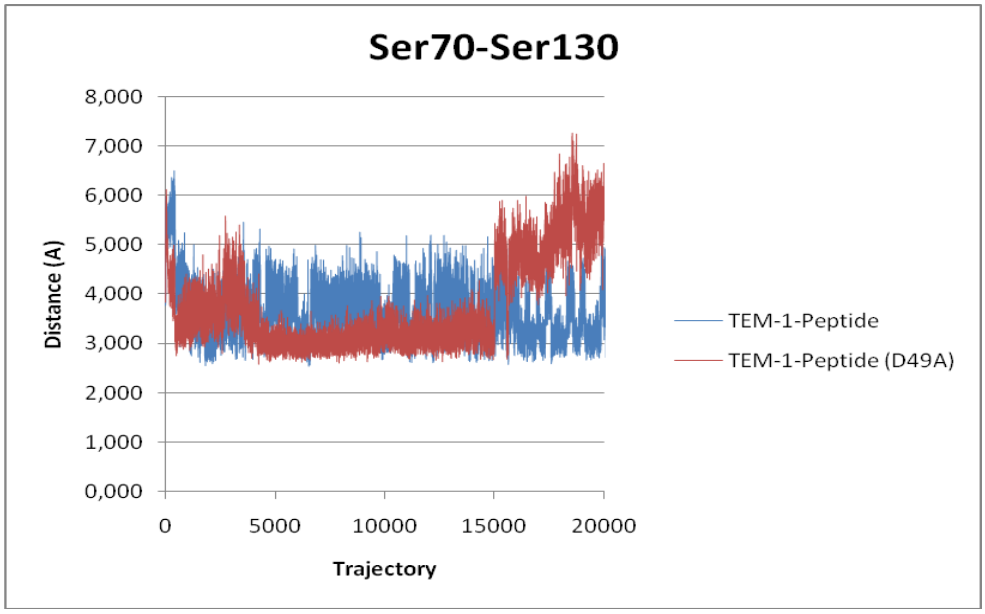

Figure B.2. Ser70 - Ser130 active site residue distances of TEM-1 – Peptide(blue) and TEM-1 – Peptide (D49A) (red) complexes.

.

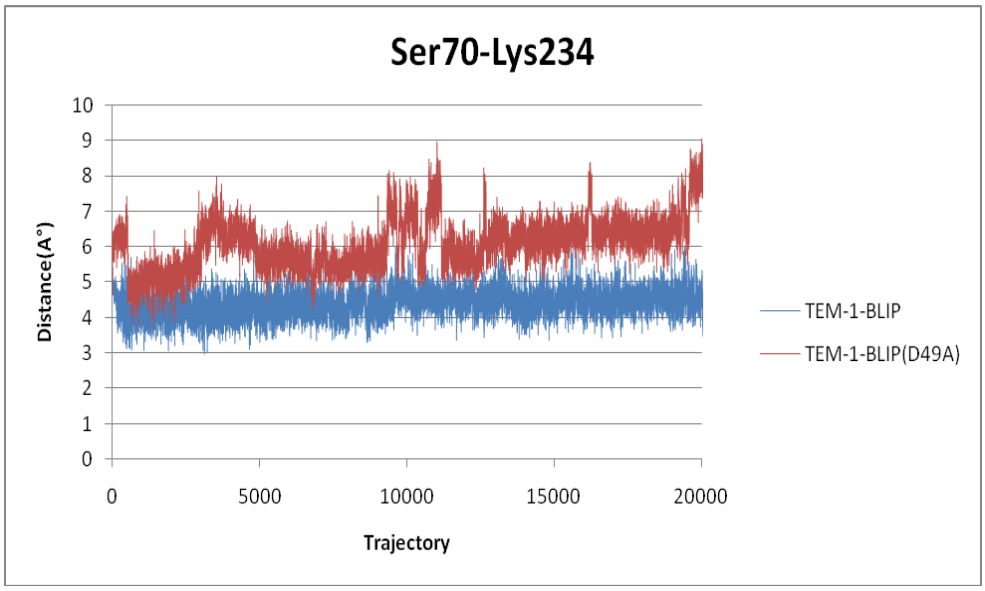

Figure B.3. Ser70 – Lys234 active site residue distances of TEM-1 – BLIP (blue) and TEM-1 – BLIP (D49A) (red) complexes.

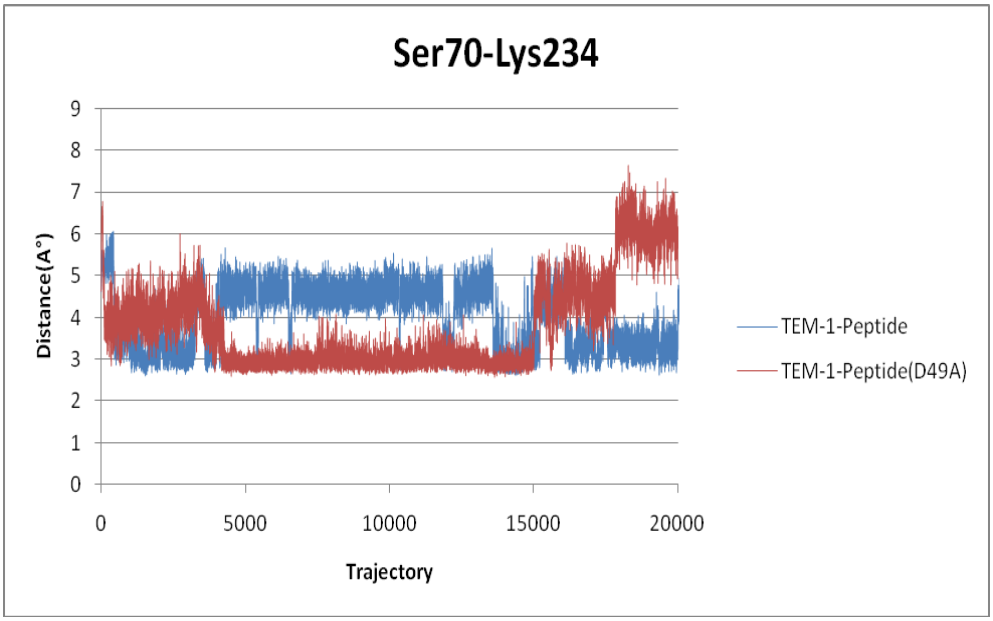

Figure B.4. Ser70 – Lys234 active site residue distances of TEM-1 – Peptide (blue) and TEM-1 – Peptide (D49A) (red) complexes.

APPENDIX C: MMPBSA RESULTS

Table C.1. Apolar Energy Values of TEM-1 BLIP and TEM-1 - BLIP (D49A) complexes

APOLAR		
Trajectory	TEM-1 - BLIP	TEM-1 - BLIP (D49A)
0	251.61	246.6
1000	226.18	222.8
5000	182.08	181.8
10000	184.83	184.1
15000	263.11	249.4
20000	248.73	233.7

Table C.2. Polar Energy Value of TEM-1 - BLIP Complex

POLAR	TEM-1 - BLIP		
Trajectory	COMPLEX	APO TEM-1	APO BLIP
0	-8371.7	-5548.5	-3153
1.000	-8727.6	-5791.4	-3126.2
5.000	-8870.5	-6062.2	-3121.1
10.000	-9215.3	-6430	-3242.7
15.000	-9246	-6267.8	-3222.3
20.000	-9458	-6343.6	-3222.3

Table C.3. Polar Energy Values of TEM-1 BLIP (D49A) Complex

POLAR	TEM-1- BLIP (D49A)		
Trajectory	TEM-1 – BLIP (D49A)	APO TEM-1	APO BLIP
0	-8137.7	-5548.5	-2967.2
1.000	-8258.6	-5791.4	-3045.7
5.000	-8782.7	-6062.2	-3024.6
10.000	-8811	-6430	-3196.4
15.000	-8955.3	-6267.8	-3274.9
20.000	-9180.9	-6343.6	-3318.8

Table C.4. Coulomb Energy Values of TEM-1 - BLIP Complex

Coulomb	TEM-1 - BLIP		
Trajectory	TEM-1 - BLIP	APO TEM-1	APO BLIP
0	-164726	-87670,8	-41649
1.000	-246183	-134819	-65257
5.000	-240088	-133186	-64551
10.000	-241380	-133837	-65067
15.000	-240853	-130621	-64948
20.000	-238846	-132776	-64492

Table C.5. Coulomb Energy Values of TEM-1 - BLIP (D49A) Complex

Coulomb	TEM-1 - BLIP (D49A)		
Trajectory	TEM-1 – BLIP (D49A)	APO TEM-1	APO BLIP
0	-163348.13	-87670.8	-47738.29
1.000	-244587.83	-134819	-74236.07
5.000	-240163.23	-133186	-73063.93
10.000	-241328.8	-133837	-73386.84
15.000	-240740.21	-130621	-73208.05
20.000	-239068.92	-132776	-72576.06

Table C.6. Internal Energy Values of TEM-1 - BLIP Complex

Internal	TEM-1 - BLIP		
Trajectory	TEM-1 - BLIP	APO TEM-1	APO BLIP
0	22396	12641	5764.2
1.000	13348	7456.9	3760.8
5.000	3215.9	1341.3	1108.1
10.000	3328.7	2121	1165.8
15.000	3432	2508.7	1226
20.000	3712	2487.4	1328.1

Table C.7. Internal Energy of Values TEM-1 - BLIP (D49A) Complex

Internal	TEM-1 – BLIP (D49A)		
Trajectory	TEM-1 – BLIP (D49A)	APO TEM-1	APO BLIP
0	22356.71	12641	6467.84
1.000	13198.92	7456.9	4200.11
5.000	3222.82	1341.3	1126.88
10.000	3358.01	2121	1174.34
15.000	3457.49	2508.7	1235.98
20.000	3727.8	2487.4	1341.11

Table C.8. Van der Waals Energy Values of TEM-1 - BLIP Complex

VDW	TEM-1 - BLIP		
Trajectory	TEM-1 - BLIP	APO TEM-1	APO BLIP
0	99999999.99	99999999.99	99999999.99
1.000	22419.52	11582.86	5713.17
5.000	26330.59	14138.15	6853.46
10.000	26376.77	13995.14	6806.3
15.000	26051.72	130040.1	6776.05
20.000	25315.39	13262.55	6597.87

Table C.9. Van der Waals Energy Values of TEM-1 - BLIP (D49A) Complex

VDW	TEM-1 BLIP (D49A)		
Trajectory	TEM-1 - BLIP	APO TEM-1	APO BLIP
0	99999999.99	99999999.99	1031886.92
1.000	21853.1075	11582.86	6718.55
5.000	26424.39	14138.15	8060.85
10.000	26521.22	13995.14	8049.71
15.000	26154.5	130040.1	7878.18
20.000	25717.69	13262.55	7567.21
	25334.1815	36603.76	7654.9

Table C.10. Delta energy values of TEM-1 – BLIP Complex

	<TEM-1 - BLIP>	<TEM-1>	<BLIP>
POLAR	-9103.48	-6179	-3186.92
vdw	22602.5976	13305.1908	7180.2368
Coulomb	-1009344.6	-556139.804	-271127.34
INTERNAL	5407.32	3183.06	1717.76

Table C.11. Delta energy values of TEM-1 – mutant BLIP (D49A) Complex

	<TEM-1 –BLIP (D49A)>	<UNBOUND TEM-1>	< BLIP (D49A)>
POLAR	-8797.7	-6179	-3172.08
vdw	22542.77344	13305.1908	7589.55912
Coulomb	-1008123.196	-556139.804	-306369.7142
INTERNAL	5393.008	3183.06	1815.684

REFERENCES

Ambler, R. P., 1980, "The structure of beta-lactamases", *Philosophical Transactions of the Royal Society*, Vol. 289, pp. 321-331

Adachi, H., T. Ohta and H. Matsuzawa, 1991, "Site-directed mutants, at position 166, of RTEM-1 beta-lactamase that form a stable acyl-enzyme intermediate with penicillin", *Journal of Biological Chemistry*, Vol. 266, pp.3186-3191.

Babic, M., A. M. Hujer, R. A. Bonomo, 2006, "What's new in antibiotic resistance? Focus on beta-lactamases", *Drug Resistance Updates*, Vol.9, pp. 142-156.

Baker, N. A., and J. A. McCammon, Electrostatic Interactions, Structural Bioinformatics, Newyork, 2003.

Cantu III, C., W. Huang, T. Palzkill, 1996, "Selection and characterization of amino acid substitutions at residues 237 ± 240 of TEM-1 beta-lactamase with altered substrate specificity for aztreonam and ceftazidime", *Journal of Biological Chemistry*, Vol. 271, pp. 22538-22545.

Cantu III, C., T. Palzkill, 1998, "The role of residue 238 of TEM-1 beta-lactamase in the hydrolysis of extended-spectrum antibiotics", *Journal of Biological Chemistry*, Vol. 273, 26603-26609.

Chen, C. C., T. J. Smith,, G. Kapadia, S. Wasch, L. E. Zawadzke, A. Coulson, O. Herzberg, 1996, "Structure and kinetics of the beta-lactamase mutants S70A and K73H from Staphylococcus aureus", *Biochemistry*, Vol. 35, pp. 12255-12258.

Cohen, S. A. And R. F. Pratt, 1980, Inactivation of Bacillus cereus beta-lactamase I by 6 beta-bromopencillanic acid: mechanism", *Biochemistry*, Vol.19, pp. 3996-4003.

Dalbadie-McFarland, G., L. W. Cohen, A. D. Riggs, C. Morin, K.Itakura, J. H. Richards, 1982, "Oligonucleotide-directed mutagenesis as a general and powerful method for studies of protein function", *Philosophical Transactions of the Royal Society*, Vol. 79, pp. 6409-6413.

Dalbadie-McFarland, G., Neitzel, J. J., Richards, J. H., 1986, "Active site mutants of beta-lactamase: use of an inactive double mutant to study requirements for catalysis", *Biochemistry*, Vol. 25, pp. 332-338.

Delmas, J., Y. Chen, F. Prati, F. Robin, B. K. Shoichet and R. Bonnet, 2008, "Structure and dynamics of CTX-M enzymes reveal insights into substrate accommodation by extended spectrum β-lactamases", Journal of Molecular Biology, Vol.375, pp. 192-201.

Diaz, N., T. L. Sordo, K. M. Merz, D. Suarez, 2003, "Insights into the acylation mechanism of Class A β-lactamase from molecular dynamics simulations of the TEM-1 enzyme complexed with Benzylpenicillin", *Journal of American Chemical Society*, Vol.125, pp. 672-684.

Doucet, N., P. - Y. Savard, J. N. Pelletier, S.M. Gagné, 1999, "NMR Investigation of Tyr^{105} Mutants in TEM-1 β-Lactamase", The Journal of Biological Chemistry, Vol.282, pp. 21448-21459.

Fisher, J., Belasco, J. G., Khosla, S., Knowles, J. R.,1980, "Beta-lactamase proceeds via an acyl-enzyme intermediate. Interaction of the Escherichia coli RTEM enzyme with cefoxitin", *Biochemistry*, Vol. 19, pp. 2895-2901.

Fogolari, F., A. Brigo and H.Molinari, 2003, "Protocol for MM/PBSA molecular dynamics simulations of proteins", *Biophysical Journal*, Vol. 85, pp. 159-166.

Frére, J. M., 1995, "Beta-lactamases and bacterial resistance to antibiotics", *Molecular Microbiology*, Vol.16, pp. 385-395.

Ghuysen, J. M., 1994, “Molecular structures of penicillin-binding proteins and beta-lactamases. Trends”, *Microbiology*, Vol.2, pp. 372-380.

Gohlke, H., C. Kiel and D. A. Case, 2003, “Insights into protein-protein binding by binding free energy calculation and free energy decomposition for the Ras-Raf and Ras-RalGDS complexes”, *Journal of Molecular Biology*, Vol. 330, pp. 891–913.

Hermann, J. C., L. Riddler, H. D. Höltje and A. J. Mulhollonad, 2006, “Molecular mechanisms of antibiotic resistance: QM/MM modelling of deacylation in a class A β-lactamase”, *Organic and Biomolecular Chemistry*, Vol.4, pp. 206-210.

Herzberg, O., J. Moult, 1987, “Bacterial resistance to beta-lactam antibiotics: crystal structure of beta-lactamase from Staphylococcus aureus PC1 at 2.5 ä resolution”, *Science*, Vol. 236, pp. 694-701.

Huang ,W., Z. Beharry, Z. Zhang and T. Pazkill, 2003, “A broad spectrum peptide inhibitor of β-lactamase identified using phage display and peptide arrays”, *Protein Engineering*, Vol. 16, pp. 853-860.

Hujer, A. M., K. M. Hujer, R. A. Bonomo, 2001, “Mutagenesis of amino acid residues in the SHV-1 beta-lactamase: the premier role of Gly238Ser in penicilin and cephalosporin resistance”, *Biochimica et Biophysica Acta*, Vol.1547, pp.37-50.

Humphrey, W. F., A. Dalke, and K. Schulten, 1996, “VMD-Visual molecular dynamics”, Journal of Molecular Graphics, Vol. 14, pp. 33.

Jayaram, B., D. Sprous, M. A. Young and D. L. Beveridge, (1998), “Free energy analysis of the conformational preferences of A and β-Forms of DNA in solution”, *Journal of American Chemical Society*, Vol. 120, pp.10629-10633.

Jelsch, C., L. Mourey, J. M. Masson and J. P. Samama, 1993, “Crystal structure of Escherichia coli TEM1 beta-lactamase at 1.8 Å”, *Proteins*, Vol. 16, pp. 364-383.

Joris, B., J. Dusart, J. M. Frere, J. van Beeumen, E. L. Emanuel, S. Petursson, J. Gagnon and S. G. Waley, 1984 , “The active site of the P99 beta-lactamase from Enterobacter cloacae”, *Biochemistry*, Vol. 223, pp. 271-274

Joughin, B. A., D. F. Gren and B. Tidor, 2005, “Action-at-a-distance interactions enhance protein binding affinity”, *Protein Science*, Vol.14, pp. 1363-1369.

Kalé, L., R. Skeel, M. Bhandarkar, R. Brunner, A. Gursoy, N. Krawetz, J. Phllips, A. Shinozaki, K. Varadarajan, and K. Schulten, 1999, “NAMD2: Greater scalability for paralel molecular dynamics” , *Journal of Computational Physics*, Vol.151, pp. 283-312.

Karplus, M., J. A. McCommon, 2002, “Molecular dynamics simulations of biomolecules”, *Nature Structural Biology*, Vol. 9, pp. 646-652.

Knott-Hunziker, V., S. Petursson, S. G. Waley, B. Jaurin and T. Grundstroem, 1982, “Structure of the wild-type TEM-1 β-lactamase at 1.55 Å and the mutant enzyme Ser70Ala at 2.1Å suggest the mode of noncovalent catalysis for the mutant enzyme”, *Biochemistry*, Vol. 207, pp. 315-322.

Kollman, P. A., I. Massova, C. Reyes, B. Kuhn, S. Huo, L. Chong, M. Lee, T. Lee, Y. Duan, W. Wang, O. Donini, P. Cieplak, J. Srinivasan, D. A. Case and T. E. III. Cheatham, 2003, “Calculating structures and free energies of complex molecules: Combining molecular mechanics and continuum models” *Accounts of Chemical Research*, Vol. 33, pp. 889-897.

Kuhn B, P. A. Kollman, 2000, “Binding of a diverse set of ligands to avidin and streptavidin: an accurate quantitative prediction of their relative affinities by a combination of molecular mechanics and continuum solvent models” *Journal of Medicinal Chemistry*, Vol. 43, pp. 3786-3791.

Kuhn, B., P. A. Kollman, 2000, “A ligand that is predicted to bind better to avidin than biotin: insights from computational fluorine scanning”, *Journal of American Chemical Society*, Vol. 122, pp. 3909– 3916.

Kuzin, A. P., M. Nukaga, Y. Nukaga, A. M. Hujer, R. A. Bonomo, J. R. Knox,1997, “Structure of the SHV-1 beta-lactamase”, *Biochemistry*, Vol. 38, pp. 5720-5727.

Laitinen, T., J. Rouvinen and M. Peräkylä, 2003, “MM-PBSA free energy analysis of endo-1,4-xylanase II (XynII)-substrate complexes: binding of the reactive sugar in a skew boat and chair conformation”, *Organic and Biomolecular Chemistry*, Vol. 1, pp. 3535-3540.

Laitinen T., J.A.Kankare and M.Perakyla, 2004, “Free energy simulations and MM-PBSA analyses on the affinity and specificity of steroid binding to antiestradiol antibody”, *PROTEINS: Structure, Function, and Bioinformatics*, Vol. 55, pp. 34-43.

Lee, T., P. A. Kollman, 2000, “Theoretical studies suggest a new antifolate as a more potent inhibitor of thymidylate synthase”, *Journal of American Chemical Society*, Vol. 122, pp. 4385- 4393.

Lee, M. R., D. Baker & P. A. Kollman, 2001, “2.1 and 1.8A average C(alpha) RMSD structure predictions on two small proteins, HP-36 and s15”, *Journal of American Chemical Society*, Vol. 123, pp. 1040-1046.

MacKerell, “Pittsburgh Supercomputing Center”, Parameter Notes, 15 Dec. 2008, <http://www.psc.edu/general/software/packages/charmm/tutorial/mackerell/PARAM_00.pdf>

Majiduddin, F. K., I. C. Materon, T. G. Palzkill, 2002, “Molecular anaylsis of beta-lactamase structure and function”, International Journal of Medical Microbiology, Vol. 292, pp.127-137.

Matagne, A., and J. M. Frere, 1995, “Contribution of mutant analysis to the understanding of enzyme catalysis : the case of class A beta-lactamases”, *Biochimica et Biophysica Acta*, Vol. 1246, pp. 109-127.

Matagne, A., J. Lamotte-Brasseur, J. M. Frere, 1998, “The catalytic properties of class A beta-lactamases : efficiency and diversity”, *Biochemistry*, Vol. 330, pp. 581-598.

Mazella, L. J., S. Pazhanisamy, R. F. Pratt, “Evidence from a mutant beta-lactamase for the mechanism of beta-lactamase-catalysed depsipeptide aminolysis”, *Biochemical Journal*, Vol. 274, pp. 55-859 (1991).

Minasov, G., X. Wang, B. K. Shoichet, 2002, “An ultrahigh resolution structure of TEM-1 β-lactamase suggests a role for Glu166 as the general base in acylation”, *Journal of the American Chemistry*, Vol. 124, pp. 5333-5340.

Page, C. S., P. A. Bates, 2006, “Can MM-PBSA calculations predict the specificities of protein kinase inhibitors?”, *Journal of Computational Chemistry*, Vol. 27, No.16, 1990-2007.

Patra, M., M. T. Hyvönen, E. Falck, M. Sabouri-Ghomi, I. Vattulainen and M. Karttunen, 2006, “Long-range interactions and parallel scalability in molecular simulations”, *Computer Physics Communications*, Vol. 176, pp. 14-22.

Petrosino, J., G. W. Rudgers, H. Gilbert, and T. Palzkill, 1999, “Contributions of Aspartate 49 and Phenylalanine 142 Residues of a Tight Binding Inhibitory Protein of beta - Lactamases”, *Journal of Biological Chemistry*, Vol. 274, pp. 2394-2400.

Pierre-Yves, S., A. Sosa-Peinado, R. C. Levesque, M. W. Makinen and S. M. Gagné, 2004, “Letter to the Editor: ^{1}H, ^{13}C and ^{15}N backbone resonance assignments for TEM-1, a 28.9 kDa β-lactamase from E. Coli”, *Journal of Biomolecular NMR*, Vol. 29, pp. 433-434.

Reading, C., and M. Cole, 1977, “Clavulanic Acid: a Beta-Lactamase-Inhibiting Beta-Lactam from Streptomyces clavuligerus”, *Antimicrob Agents Chemother*, Vol. 11, pp.852-857.

Roccatano, D., G. Sbardella, M. Aschi, G. Amicosante, C. Bossa, A.D. Nola and F. Mazza, 2005, “Dynamical aspects of TEM-1 β-lactamase probed by molecular dynamics”, *Journal of Computer-Aided Molecular Design*, Vol. 19, pp. 329-340.

Rudgers, G. W., T. Palzkill, 1999, “Identification of residues in β-lactamase critical for binding β-lactamase inhibitory protein”, *The Journal of Biological Chemistry*, Vol. 274, pp. 6963-6971.

Rudgers, G. W., W. Huang and T. Palzkill, 2001, “Binding Properties of a Peptide Derived from β-lactamase Inhibitory Protein”, *Antimicrobial Agents and Chemotherapy*, Vol. 45, pp. 3279-3286.

Selzer, T., S. Albeck and G. Schreiber, 2000, “Rational design of faster associating and tighter binding protein complexes”, *Nature Structural Biology*, Vol. 7, pp. 537-541.

Srinivasan, J., T. E: Cheatham, P. III, Cieplak, P. A. Kollman & D. A. Case, 1998, “Continuum solvent studies of the stability of DNA, RNA and phosphoramidate-DNA helices”, *Journal of American Chemical Society*, Vol. 120, pp. 9401-9409.

Stec, B., K. M. Holtz, C. L. Wojciechowski and E. R. Kantrowitz, 2005, “Structure of the wild-type β-lactamase at 1.55A˚ and the mutant enzyme Ser70Ala at 2.1A˚ suggest the mode of the noncovalent catalysis fort he mutant enzyme”, *Acta Crystallographica*, Vol. 61, pp. 1072-1079.

Stratagene, “Stragene” pET System Vectors and Hosts, Instruction Manual, 20 Dec. 2008 <http://www.stratagene.com/manuals/211521.pdf>

Strynadka, N. C. J., H. Adachi, Jensen S. E., K. Johns, A. Sielecki, C. Betzel, K. Sutoh and M. N. G. James, 1992, "Molecular structure of the acyl-enzyme intermediate in β lactam hydrolysis at 1.7A˚ resolutions", *Nature*, Vol. 359, pp. 700-705.

Strynadka, N. C., Jensen S. E., P. M. Alzari and M. N. G. James, 1996, "A potent new mode of beta-lactamase inhibition revealed by the 1.7 Å X-ray crystallographic structure of the TEM-1-BLIP complex.", *Nature Structural Biology*, Vol. 3, pp. 290-297.

Sun, W., Y. Hu, J. Gong, Zhu and B. Zhu, 2005, "Identification of b–lactamase Inhibitory Peptide Using Yeast Two-Hybrid System", *Biochemistry*, Vol. 70, pp. 753-760.

Venkatachalam, K. V., Huang, W., LaRocco, M., Palzkill, T., 1994, "Characterization of TEM-1 beta-lactamase mutants from positions 238 to 241 with increased catalytic efficiency for ceftazadime" *Journal of Biological Chemistry*, Vol.269, 23444-23450.

Vorobjev, Y. N., J. C. Almagro and J. Hermans, 1998, "Discrimination between native and intentionally misfolded conformations of proteins: ES/IS, a new method for calculating conformational free energy that uses both dynamic simulations with explicit solvent, and an implicit solvent continuum model" *Proteins*, Vol. 32, pp. 399-413.

Wang, J., P. Morin, W. Wang and P. A. Kollman, 2001, "Use of MM-PBSA in reproducing the binding free energies to HIV-1 RT of TIBO derivatives and predicting the binding mode to HIV-1 RT of efavirenz by docking and MM-PBSA", *Journal of American Chemical Society*, Vol. 123, pp. 5221-5230.

Wilke, M. S., A. L. Lovering and N. C. Strynadka, 2005, "B-Lactam antibiotic resistance: a current structural perspective", *Current Opinion in Microbiology*, Vol. 8, pp. 525-533.

Zhang, Z., and T. Palzkill, 2003, "Determinants of binding affinity and specificity for the interaction of TEM-1 and SME-1 β-Lactamase with β-Lactamase inhibitory protein β-Lactamases", *The Journal of Biological Chemistry*, Vol. 278, pp. 45706–45712.

Zhang, Z., and T. Palzkill, 2004, "Dissecting the protein-protein interface between β-lactamase inhibitory protein and Class A β-lactamases", *The Journal of Biological Chemistry*, Vol. 279, pp. 42860–42866.